

**NUMERICAL ANALYSIS OF RAILWAY FORMATION WITH GEOGRID
REINFORCED BALLAST AND BLANKET LAYER FOR HIGH-SPEED
RAIL**

A DISSERTATION

SUBMITTED IN PARTIAL FULFILLMENT OF THE REQUIREMENTS FOR
THE AWARD OF THE DEGREE OF

**MASTER OF TECHNOLOGY
IN
GEOTECHNICAL ENGINEERING**

Submitted by:

VEER VIKRAM SINGH

(2K21/GTE/19)

Under the supervision of

PROF. A. K. SAHU



DEPARTMENT OF CIVIL ENGINEERING

DELHI TECHNOLOGICAL UNIVERSITY

(Formerly Delhi College of Engineering)

Bawana Road, Delhi-110042

MAY, 2023

DELHI TECHNOLOGICAL UNIVERSITY
(Formerly Delhi College of Engineering)
Bawana Road, Delhi – 110042

CANDIDATE'S DECLARATION

I, VEER VIKRAM SINGH, 2K21/GTE/19, of MTech (Geotechnical Engineering), hereby declare that the project Dissertation titled “ Numerical Analysis of Railway Formation with Geogrid Reinforced Ballast and Blanket Layer for High-Speed Rail” which is submitted by me to the Department of Civil Engineering, Delhi Technological University, Delhi in partial fulfilment of the requirement for the award of the degree of Master of Technology, is original and not copied from any source without proper citation. This work has not previously formed the basis for the award of any Degree, Diploma Associateship, Fellowship, or other similar title or recognition.

Place: Delhi

VEER VIKRAM SINGH

Date:

DELHI TECHNOLOGICAL UNIVERSITY

(Formerly Delhi College of Engineering)

Bawana Road, Delhi – 110042

CERTIFICATE

I hereby certify that the Project Dissertation titled “Numerical Analysis of Railway Formation with Geogrid Reinforced Ballast and Blanket Layer for High-Speed Rail” which is submitted by VEER VIKRAM SINGH, 2K21/GTE/19, Department of Civil Engineering, Delhi Technological University, Delhi in partial fulfilment of the requirement for the award of the degree of Master of Technology, is a record of the project work carried out by the student under my supervision. To the best of my knowledge, this work has not been submitted in part or full for any Degree or Diploma to this University or elsewhere.

Place: Delhi

ANIL KUMAR SAHU

Date:

SUPERVISOR & PROFESSOR

Department of Civil Engineering
Delhi Technological University
Bawana road, Delhi – 110042

ABSTRACT

India will launch a high-speed rail project to improve the travel time between cities in the upcoming years. Upgrading its current speed of 180 km/h to a high speed of 360 km/h will be a turning point in railway transportation. The Vande Bharat Express is the current high-speed train that travels at a speed of 180 km/hr. India intends to start its first bullet train by 2026. But as the travel speed increases, the stresses will increase on the existing soil formation. The strains on India's railway subgrade component would significantly rise with the addition of high-speed railways and bullet trains. The strains may cause failure in more brittle soil. For thousands of years, soils are mixed with different fibers, fabrics, and vegetation to improve quality and stability. Geosynthetics which are polymer products are used in Civil engineering for decades. Utilizing geo-synthetics in the lengths of currently weak formations is an alternate strategy to reduce the number of stress.

This paper gives a numerical analysis of the behavior of railway embankments built on sand. Finite element software was used to simulate the model. Using the finite element software PLAXIS 3D, a railway embankment's vertical deformations and stresses are calculated under a moving train load of 90 kN. The speeds of the moving train are taken as 180 km/h and 360 km/h for the modeling. Geogrid is installed as per the recommendations by RDSO (2018). The blanket layer and ballast layer are reinforced with geogrids at different depths. It was observed that on using geogrid in the different layers, the deformations and the stresses could be reduced up to certain levels. After analyzing the model, it can be concluded that Geogrids are beneficial in restricting the deformations and the stresses at particular sections but further studies are required to check the suitability of geogrids for the long run.

ACKNOWLEDGEMENT

I would like to offer my heartfelt appreciation to everyone who helped me finish this academic project. This initiative would not have been feasible without their assistance and support.

First and foremost, I would want to thank Hon. Vice Chancellor **Prof. J.P. Saini** (Delhi Technological University), **Dean Academics PG** section, for providing me the platform to complete my research. I appreciate the believe and faith the university has put into me.

I would like to thank **Prof. V K Minocha** (Head of the Department, Delhi technological university) and **Prof. A.K. Sahu** (Delhi Technological University) my academic project supervisor for motivating and inspiring me throughout this journey, and for their brilliant comments and suggestions.

I also want to thank my family and friends for their constant support and encouragement during this effort. Their faith in me has been both motivating and inspiring.

Finally, I'd want to thank God for allowing me to go through all of this. Day by day, I've felt your leadership. You are the one who allowed me to complete my degree. I will continue to put my faith in you for my future.

VEER VIKRAM SINGH
(2K21/GTE/19)

CONTENTS

Candidate's declaration	i
Certificate	ii
Abstract	iii
Acknowledgment	iv
Content	v
List of Tables	vii
List of Figures	viii
List of Symbols and Abbreviations	x
CHAPTER 1- INTRODUCTION	
1.1 General	1
1.1.1 Railway formation	2
1.1.2 Ballast and its function	3
1.1.3 Blanket and its function	3
1.1.4 Subgrade and its function	4
1.2 Geosynthetic materials	5
1.2.1 Functions of geosynthetics	5
1.2.2 Various types of geosynthetics	8
1.2.3 Use of geosynthetic in railway engineering	11
1.3 Finite element model	12
1.4 Objectives of the Research	14
1.5 Overview of Thesis	14
CHAPTER 2- LITERATURE REVIEWS	
2.1 General	15

2.2 Research Gap	22
CHAPTER 3- METHODOLOGY	
3.1 General	23
3.2 Modeling	24
3.3 Material properties	25
3.3.1 Geogrids	26
3.4 Simulation	27
3.4.2 Plaxis 3D	27
3.4.2 Finite element model	28
3.4.3 Loading	30
3.5 Meshing	31
CHAPTER 4- RESULTS AND DISCUSSION	
4.1 General	33
4.2 For Model 1	33
4.2.1 Vertical deformations	33
4.2.2 Displacements and stress in the rail section	38
4.3 For Model 2	41
4.3.1 Vertical deformations	41
4.3.2 Stress in the section	44
4.3.3 Displacement and stress in the rail section	45
CHAPTER 5- CONCLUSIONS	48
REFERENCES	49

LIST OF TABLES

Table 1.1	GRADATION AND SIZE	3
Table 1.2	PROPERTIES OF FORMATION LAYERS	4
Table 3.1	BASIC MATERIAL CHARACTERISTICS OF THE SOIL LAYERS FOR LE AND MC MODELS	25
Table 3.2	INPUT PROPERTIES IN PLAXIS 3D FOR RAIL AND SLEEPER	25
Table 3.3	PROPERTIES OF GEOGRIDS	26
Table 3.4	MODEL PARAMETERS FOR MODELING THE MOVING LOADS	28
Table 4.1	DEFORMATIONS IN THE Z-DIRECTION WITH AND WITHOUT GEOGRID	34
Table 4.2	DEFORMATIONS IN THE Y-DIRECTION WITH AND WITHOUT GEOGRID	37

LIST OF FIGURES

Fig 1.1	Railway Formation and Geometry (RDSO 2018)	1
Fig. 1.2	Separation of layers	2
Fig. 1.3	Filtration	5
Fig. 1.4	Drainage	6
Fig. 1.5	Reinforcement	7
Fig. 1.6	Geotextiles	7
Fig. 1.7	Types of geogrids	8
Fig. 1.8	Geomembrane	9
Fig. 1.9	Geonets	9
Fig.1.10	Geofoams	10
Fig. 1.11	Geosynthetic in prepared subgrade	11
Fig. 1.12	Typical two-dimensional finite elements	11
Fig 3.1	Flow chart of the methodology	12
Fig. 3.2	Dimensions of the numerical model	23
Fig. 3.3	Railway section for the modeling	24
Fig. 3.4	Dimensions of an ICE train and calculated lengths for model	24
Fig. 3.5	Finite element model	28
Fig. 3.6	Illustration of loading	29
Fig. 3.7	Elements and nodes for Model 1	30
Fig. 3.8	Elements and nodes for Model 2	31
Fig 4.1	The graph between deformation and time at speed 180 km/h.	32
Fig 4.2	The graph between deformation and time at 360 km/h.	34
Fig. 4.3	Total displacements at different intervals without the geogrid	35
Fig. 4.4	Total displacements at different intervals with the geogrid	35
Fig 4.5	The graph between deformation and time at speed 180 km/h.	36
Fig 4.6	The graph between deformation and time at speed 360 km/h.	37

Fig 4.7	Axial force(kN) and the cross-section of the rail (m)	38
Fig 4.8	Axial force(kN) and the cross-section of the rail (m)	38
Fig 4.9	Plot between displacement(m) and cross-section of the rail (m)	39
Fig 4.10	Plot between displacement(m) and cross-section of the rail (m)	39
Fig 4.11	Shear forces in the x-y direction	40
Fig 4.12	Shear forces in the x-z direction	40
Fig. 4.13	Total displacement without the geogrid	41
Fig. 4.14	Total displacements with the geogrid	42
Fig. 4.15	Total displacement without the geogrid	42
Fig. 4.16	Total displacement with the geogrid	43
Fig. 4.17	Vertical stress at time=0.1 sec without the geogrid	43
Fig. 4.18	Vertical stress at time=0.1 sec with the geogrid	44
Fig 4.19	Plot between axial force(kN) and cross-section of the rail (m)	44
Fig 4.20	Plot between axial force(kN) and cross-section of the rail (m)	45
Fig.4.21	Plot between displacement(m) and cross-section of the rail (m)	45
Fig.4.22	Plot between displacement(m) and cross-section of the rail (m)	46
Fig.4.23	Plot between total displacement(m) and cross-section of the rail (m) at speed 180 km/h.	47
Fig.4.24	Plot between total displacement(m) and cross-section of the rail (m) at speed 360 km/h.	47

LIST OF SYMBOLS AND ABBREVIATIONS

Abbreviations/Symbols	Descriptions
RDSO	Railway design and standard organization
GC	Clayey Gravel
SM	Silty Sand
SC	Clayey Sand
SM-SC	Clayey silty sand
CBR	California Bearing Ratio
MDD	Maximum Dry Density
FEM	Finite Element model
FEA	Finite element analysis
LE	Linear Element model
MC	Mohr Coulomb's model
γ_{sat}	Saturated unit weight (kN/m ³)
γ_{unsat}	Unsaturated unit weight (kN/m ³)
μ	Poisson's ratio
ϕ	Angle of friction
c	Cohesion (kN/m ²)
Ψ	Dilatancy angle
E	Young's Modulus (kN/m ²)

CHAPTER 1

INTRODUCTION

1.1 GENERAL

An essential component of India's transportation infrastructure is the railway track system. Because of the country's economic development, the railroads must increase their capacity to handle more traffic by installing higher axles larger payloads, and faster speeds. This necessitates the use of an improved superstructure and substructure track system. The strength of a track's foundation has a major impact on how well it performs. Its establishment should be suitably designed to accommodate upcoming moving loads and created using current and relevant techniques to have low maintenance requirements and acceptable riding quality. Under the current level of traffic, already lengthy formations that were built later as well as recently are displaying signs of difficulty. As bigger axle weights and high-speed rails are introduced the formation lengths are anticipated to grow exponentially.

1.1.1 RAILWAY FORMATION

Generally, the formation is a crucial component of the track. It enables the following purposes: (a) It offers a uniform and smooth surface on which for laying the track. (b) It supports the moving load transmits to it through the ballast. (c) It makes drainage easier. (d) It gives the track stability.

Formations typically consist of the ballast, the blanket layer, the constructed subgrade, and the embankment heap. Based on the soil's exploitability and monetary prerequisites, formations can be Single- or two-layer. Figure 1 explicates the single-layer construction of the railway formation.

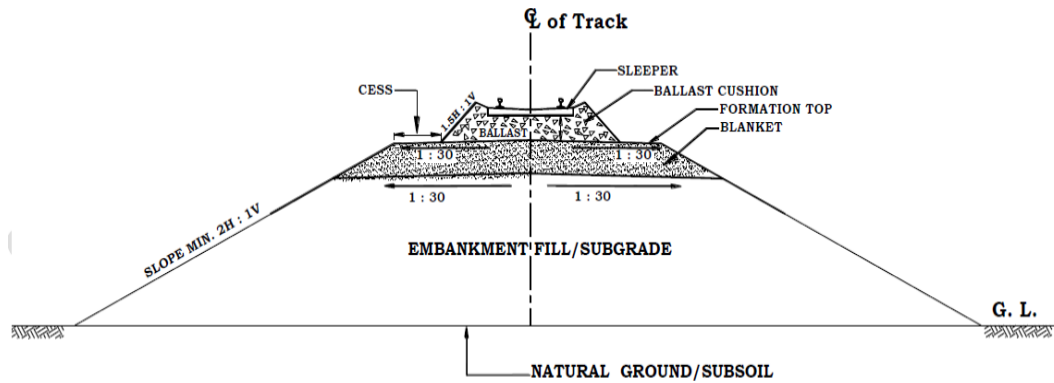


Fig 1.1 Railway formation and geometry (RDSO 2018)

The components of Railway formations are:

BALLAST: Suppressed stone with required/desired designation layered just underneath the sleepers.

SUB-BALLAST: Sub-ballast consists of a surface of coarse granulated substance arranged between the blanket and the ballast. Indian Railway does not use sub-ballast generally.

BLANKET: The blanket layer consists of coarse, granular material of designed thickness provided between the ballast and subgrade.

SUBGRADE: Subgrade is the topmost part of the filling designed with abstracted soil of desired specification.

SUBSOIL: The soil below natural ground level.

The following requirements must be met to build an establishment that provides distress-free service even in the worst possible loading, maintenance, and weather conditions:

- i. A bank or cutting subgrade should be robust in order to avoid shear strength failure under load and burden loads.
- ii. Second, any deformation caused by compression and unification in the subgrade and stratum must be within acceptable restraints.

1.1.2 BALLAST AND IT'S FUNCTIONS:

The ballast is a granular substance stationed and packed beneath and around the railway sleepers. Ballast's primary assignment is to transport load from the sleepers to the bottom surface and to facilitate a drainage channel for the track. The following are the purposes of ballast:

- a. It provides an even bed or support for railway sleepers.
- b. It moves the weight from the sleepers to the subgrade and evenly distributes it.
- c. While the trains pass by, it maintains the sleepers' stable positions.
- d. It stops sleepers from moving laterally and longitudinally.
- e. It provides the track with good drainage.

RDSO (2018) has recommended size, gradations, rock types, and other properties of aggregate used for ballast as summarized in **Table 1.1**.

Table 1.1 GRADATION AND SIZE

Retained on 65mm sq. mesh sieve	5% Maximum
Retained on 40mm sq. mesh sieve*	40%-60%.
Retained on 20mm sq. mesh sieve	Not less than 98% for machine crushed Not less than 95% for hand broken

* For machine-crushed ballast only

1.1.3 BLANKET AND IT'S FUNCTION:

When building additional lines, permanent detours, or increasing the formation, a suitable blanket thickness must always be given to guard against swelling and contracting and to avoid track formation failure due to insufficient load capacity. The followings are the needs and provisions for the blanket layer.

- a) It reduces subgrade failures under extreme critical situations such as precipitation, drainage, track servicing, and traffic loads.

- b) It blocks ballast from penetrating the subgrade and fine particle migration upward from the subgrade into the ballast under challenging circumstances.
- c) Lack of it or insufficient thickness causes instability and the creation of yields. High maintenance inputs are required as a result, which raises maintenance costs.
- d) Without it, the subgrade soil may lose its bearing ability and eventually shear, jeopardizing the safety of oncoming vehicles.
- e) It prevents subgrade plastic deformation brought on by moving loads' cyclic stresses.

The soils which required at least 60cm deep Blanket are Clayey Gravel (GC), Silty Sand (SM), Clayey Sand (SC), and Clayey Silty sand (SM-SC).

1.1.4 SUBGRADE AND ITS FUNCTION:

The sub-grade course normally consists of natural soil and aggregate of a particular particle size that has been compacted to a set degree to withstand the relative stress caused by the weight of the course above. Any weight or load stress communicated from the courses above can (or should be able to) be absorbed by this course. Soft and sinking tracks, mud leaking into the ballast, gushing ties, ballast piercing into the subgrade, the creation of water-filled ballast pouches, slips, and even total failure are all indicators of an inadequate subgrade. **Table 1.2** describes the limiting values of the different formation layers.

Table 1.2 Properties of Formation Layers

Layer	Limiting properties
Embankment fill Top layer(subgrade)	CBR>7 but not <6(compacted at 98% of MDD) Min. E_{v2} = 45 MPa CBR \geq 3(compacted at 98% of MDD)
Lower fill	
Ground/sub-soil	C_u > 25 KPa or N >5 or min. E_{v2} = 20 MPa Ground treatment is required if E_{v2} < 20 MPa

1.2 GEOSYNTHETIC MATERIALS

Geosynthetic materials created by humans are used to improve soil quality. The word is made up of the following two words: Geo, which means "earth" or "soil," and Synthetics, which means "man-made." Polymers (sometimes known as "plastics") derived from chemicals are typically used to create geosynthetic materials. Geosynthetic materials are used in geotechnical, transportation, hydraulic, and other civil engineering-related fields.

1.2.1 FUNCTIONS OF GEOSYNTHETIC

Related to railway applications, the functions of geosynthetic materials are:

(a) SEPARATION

Geosynthetics can be used to separate railway support structure layers with varying particle sizes and characteristics. It inhibits the combining of two soil types while keeping the integrity of each substance (Fig.1.2). Furthermore, geosynthetics can limit granular particles from penetrating a soft subgrade, preserving the closeness and wholeness of the granular layering and thus increasing track lifetime.

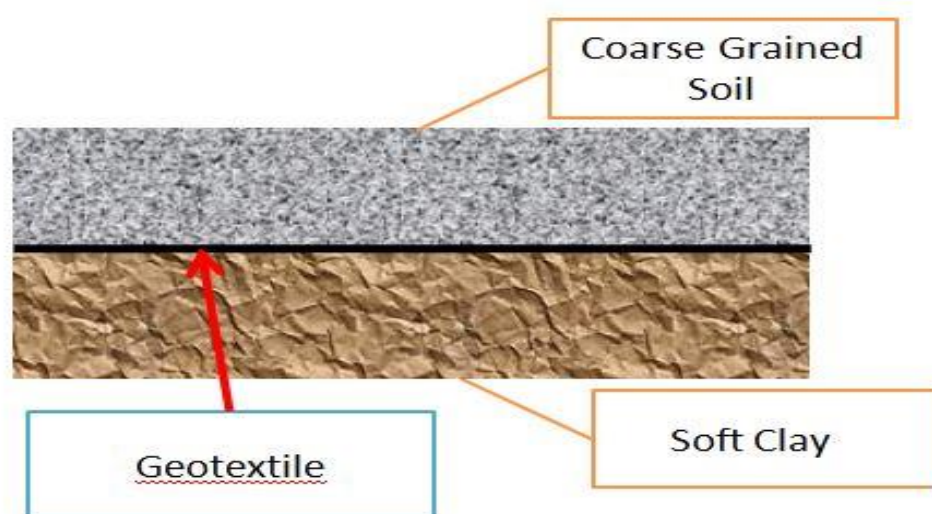


Fig. 1.2 Separation of layers

(b) FILTRATION

Water flowing from the subgrade into the granular layers above may contain particles from the subgrade. This happens due to an increase in stress levels in the subgrade caused by train passing. In this situation, a geosynthetic (geotextile) can function as a filter, enabling water to pass freely but retaining subgrade solid particles. The geotextile must have enough permeability, retention, and clogging resistance to perform this role. Fig.1.3 illustrates the filtration process.

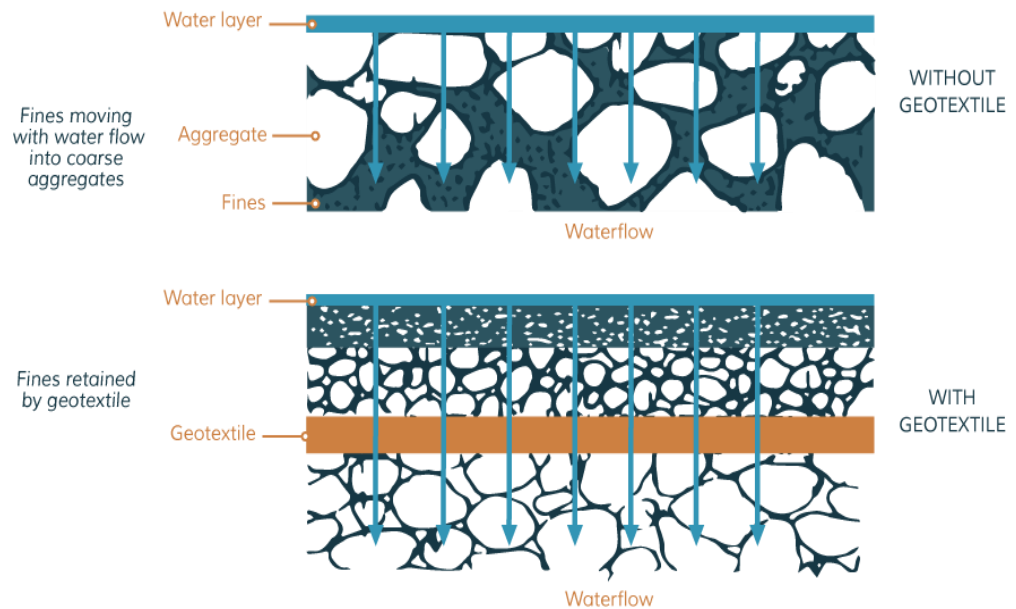


Fig. 1.3 Filtration

(c) DRAINAGE

Good drainage is critical for minimizing track damage attributed to water generated on the track from precipitation or injected from the subsoil through the ballast coverings. A seepage geosynthetic placed at certain points across the track organization can offer cross-track seepage, arresting water collection. The geosynthetic must have a significant discharge capacity in this

application. Fig. 1.4 describes the working of drainage process of geosynthetic.

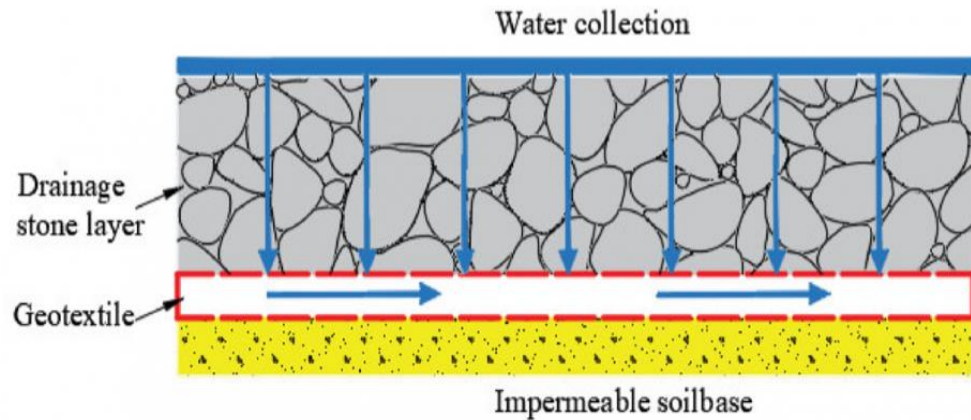


Fig. 1.4 Drainage

(d) REINFORCEMENT

Geosynthetics put over unstable subgrades may obviate the need to replace the soil, enhancing the system's load-bearing capability due to improved stress distribution. Geosynthetics installed in the ballast or secondary-ballast coatings may assist to prevent settlements caused by the sideways broadening of the ballast and sub-ballast materials (Fig.1.5). The key geosynthetic properties that must be addressed for this assignment are the interaction linking geosynthetic and soil/ballast, mechanical damage protection, tensile rigidity modulus, and tensile strength.

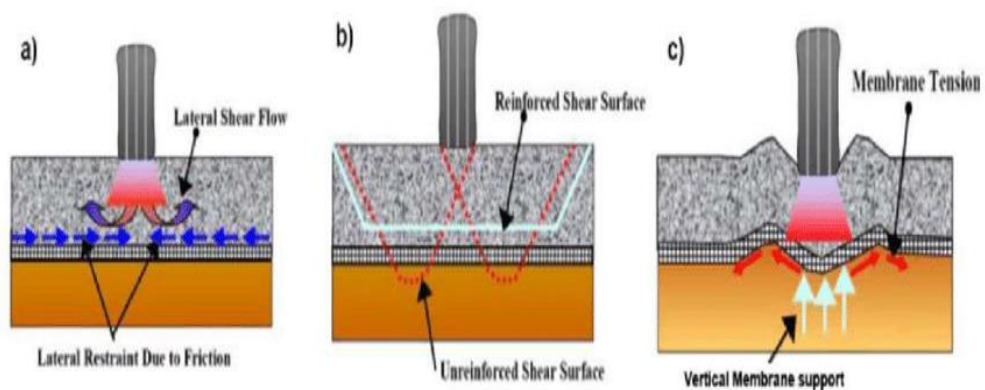


Fig. 1.5 Reinforcement

1.2.2 VARIOUS TYPES OF GEOSYNTHETICS

1.2.2.1 GEOTEXTILE

Geotextiles are permeable, planar pieces employed in civil engineering projects with soil/boulder and/or additional geotechnical particulars. They are essential fabrics made from synthetic fibers (Fig.1.6). As a result, decomposition does not pose a problem for geotextiles. Geotextiles are made from polypropylene, polyester, polyethylene with a high density, and polyamide (nylon), or a mix of these polymers. but the majority of geotextiles are created from Polypropylene. They are of woven and non-woven types.



Fig. 1.6 Geotextiles

1.2.2.2 GEOGRID

Geogrids transmit loads equally across a larger area by stiffening the foundation, which resists flexural deformation. Geogrids are synthetic equal structures made up of a well-structured matrix of tensile components with Large enough holes for interlocking with adjacent soil, rock, earth, or additional geotechnical components. All geogrid openings are big enough to enable soil interaction or crossed out from one side to the other. Geogrids are made of polymers with high

modulus and low creep sensitivity. Fig.1.7 shows different types of geogrids available in the market.

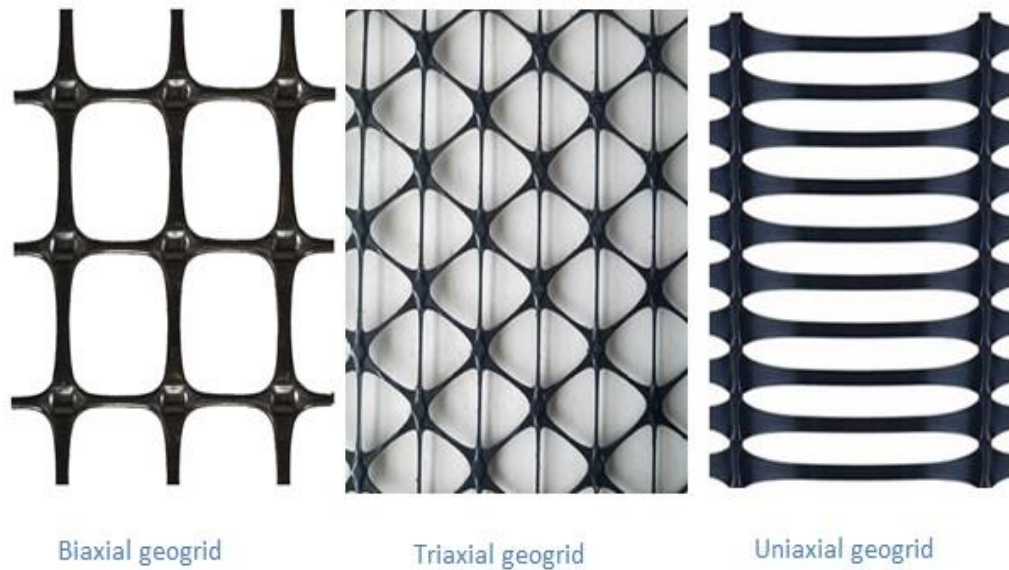


Fig. 1.7 Types of Geogrids

1.2.2.3 GEOMEMBRANES

Geomembranes are small-penetrable vinyl beddings with thicknesses ranging from 0.5 to 3 mm that are regularly acclimated for the cushioning and coverings of rigid or fluid deposit amenities. Geomembranes are very non-perforable and control fluid gesticulation. Fig.1.8 shows a typical geomembrane.



Fig. 1.8 Geomembrane

1.2.2.4 GEONETS

Geonets and Geospacers are structured similarly to Geogrids. Geonets are composed of an uninterrupted horizontal series of polysynthetic segments that are at 90° orientations to each other and generate a net-like structure. (Fig.1.9). Welding threads/bands or squeezing thermoplastic resins are used to create them.



Fig. 1.9 Geonets

1.2.2.5 GEOFOAMS

Geofoams are chunks or coverings made by enlarging polystyrene insulation to shape a low-density matrix of adjacent, gas-filled compartments. (Fig.1.10). They are feathered and can tolerate extreme circumstances. Geofoams are also acclimated as a stuffed material to diminish lateral forces on retaining partitions and loads on intrinsic soils, foundations, and abutments. They are quite popular due to their inexpensive value and improved eco-friendly sustainability.



Fig.1.10 Geofoms

1.2.3 USE OF GEOSYNTHETICS IN RAILWAY ENGINEERING

Geosynthetics can be used for the following railway embankment applications [21]:

- a. Constructing a new elevation using fine-grained soils.
- b. In the scenario of soft subsoils, upgrading the ground.
- c. Building a new elevation over soft underlying soil.
- d. Reducing the depth of the blanket/granular substance layer during the establishment of the new embankment.
- e. Rehabilitation/reinforcing of frail/Unstable Formations.
- f. Reinforced Earth Embankment/Slope Construction.
- g. Side slope erosion control.
- h. Drainage behind the bridge abutment/retaining wall.

Fig. 1.11 shows the placement of the geosynthetic over the embankment fill.

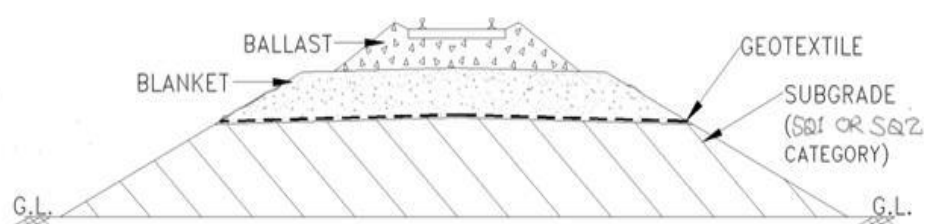


Fig. 1.11 Geosynthetic in prepared subgrade

1.3 FINITE ELEMENT METHOD

The finite element method (FEM) is a calculable procedure for forecasting the pattern of an establishment by doing a finite element analysis (FEA) of any provided physical phenomena. FEM is a rough estimation method that divides a complex space or sector into tiny, measurable, and bounded components (hence the term finite elements) whose behavior can be described using relatively simple equations.

The finite element method involves the following steps:

i. Discretization of elements:

This is the technique of modeling the geometry of the topic under consideration using a collection of small regions known as finite elements. The geometry is defined by the coordinates of important places on the element known as Nodes. These elements have nodes defined on or within the element boundaries. These nodes are generally found near the corners of elements with straight sides. Fig. 1.12 shows typical two-dimensional finite elements.

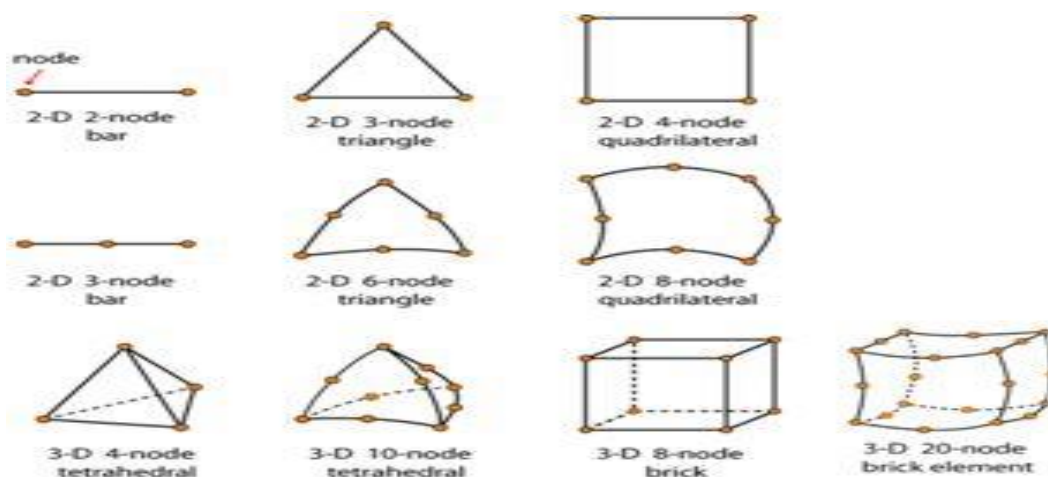


Fig. 1.12 Typical two-dimensional finite elements

ii. Approximation of the primary variable:

A primary variable (e.g., displacements, stresses, etc.) must be chosen, and criteria for how it should vary across a finite element must be specified. This variation is represented by nodal values. Displacements are commonly used as the key variable in geotechnical engineering.

The conventional three-dimensional finite element analysis approaches are the same as those used in two-dimensional models. The only difference is that the entire domain must be considered rather than a two-dimensional slice of the original boundary value problem. This entails converting the problem's geometry into a collection of three-dimensional finite elements. Tetrahedra and hexahedra are the two most common elements.

The mainly used software used in Geotechnical engineering for simulation are:

1. PLAXIS (2D/3D)
2. GEOSTUDIO (2D/3D)
3. FLAC (2D/3D)
4. ABAQUS (2D/3D)
5. MIDAS (2D/3D)

1.4 OBJECTIVES OF THE RESEARCH

The primary aspirations of the research study are:

- ✚ To develop a 3D model of a railway substructure based on the specifications provided.
- ✚ To simulate the dynamic conditions on the developed model.
- ✚ To analyze the model with the help of the numerical modeling software PLAXIS (3D).
- ✚ To analyze the model for different speeds of moving load.
- ✚ To analyze the effect of using geosynthetics in the substructure.
- ✚ To compare the suitability of geosynthetics on different subgrade layers of Railway substructure.

1.5 OVERVIEW OF THESIS

Chapter 1- highlights the subject with additional information about materials, modeling, and the objective of the study.

Chapter 2- discusses the previous works done by the researchers in the form of a literature review.

Chapter 3- discusses the methodology, simulation, and model used.

Chapter 4- discusses the results obtained from the above work

Chapter 5- discusses the inferences extracted from the above study and also discusses some recommendations.

CHAPTER 2

LITERATURE REVIEW

2.1 GENERAL

This portion incorporates earlier research completed by previous researchers to understand the dynamic behavior involving moving loads along with the applications of geosynthetics on the substructure of the railway embankment. Dynamic behavior analysis is important for moving loads as the parameters' distribution differs from static loading.

Zhu et al. (2018) investigated the identification of Railway Ballasted route Systems from In-Service Train Dynamic Responses. Using dynamic data on in-service vehicles, this study employed an adaptive regularisation technique to discover the characteristics of a railway ballasted line network (substructure). The vehicle-track interaction network was theoretically described as a discrete spring-mass simulation with a Winkler elastic foundation. The rail was designed as an indefinitely long beam supported by individual springs.

Chen et al. (2015) investigated the probabilistic analytical methodology for assessing the settling risk of a high-speed railway subgrade. In the study, an analytical model was suggested to anticipate the progressive settling of a fast rail subgrade while considering the influence of the starting stress situation. Dynamic load triaxial experiments were performed to determine the elements involved in the analytical model. Full-scale simulations were conducted to authenticate the capabilities of the suggested computer model to anticipate the cumulative settlement of a rapid rail subgrade.

Zhang et al. (2016) utilized the discrete element technique to introspect the dynamic behavior of high-paced railway ballast under moving vehicular loads. Utilizing the locomotive vehicle-track linked moving wheel loads dynamics simulation as agitated inputs, the discrete element representation was utilized to simulate the dynamic behavior of ballast granules as a result of an interaction effect, stress, and vibration reaction. The amplitudes of ballast particle vibration accelerated with the pace of the vehicle, and acceleration magnitudes rose fast after the vehicle speed approached 200 km/h.

Leng et al. (2017) used huge-scale undrained cyclic triaxial experiments to inspect the durable and displacement characteristics of massive railway embankment substances. According to research, the crucial cyclic stress (CCS) value influences cumulative irreversible (or plastic) deformation significantly. The study presented the results of a number of persistent-load, chocked, continuous deformation triaxial experiments carried out in the lab utilizing specialized heavy-scale triaxial equipment. CGS samples with varied amounts of dampness were tested for a variety of confining and deviator stress intensities.

Sun et al. (2015) investigated the deformation and deterioration mechanisms of railway ballast due to excessive-frequency cyclic stress. A series of massive cyclic triaxial experiments were performed to scrutinize the effects of train movement (frequency), wheel burden, and containment on ballast distortion and deterioration. In stated studies, the force-frequency (f) was modified from 5 to 60 Hz to mimic train pace that varied from 40 to 400 km/h. The effect of three levels of confinement pressure σ_3' (10, 30, and 60 kPa) on axle burdens of 25 and 40 t was tested utilizing two different series of deviating stress intensity $q_{\max, cyc}$ (230 and 370 kPa).

Ntotsios et al. (2019) studied the ground vibration caused by ballasted and slab railroads. The purpose of this effort was to use statistics to assess the variations between concrete tracks and ballasted tracks MOTIV (Modelling of train-induced vibration) model. It was a three-dimensional universal and fully connected model that worked in the wavenumber-frequency domain. It could anticipate rail and surface vibration levels generated by a passing train's gravitational loading, as well as axle and rail irregularities.

Grossoni et al. (2021) studied the vehicle-track interaction analysis, in the modeling of railway ballasted track settling. The research established a semi-analytical approach for calculating plastic settlements of the track bed with train passing based on recognized granular substance behavior with cyclic loading. The semi-analytical framework was then combined with a vehicle-track contact assessment to compute the rates of long-term settlement growth for varied starting track surface stiffnesses, vehicle types, and rates.

Ruiz et al. (2021) conducted a numerical investigation on crucial length to investigate the enhancement of the crucial speed in high-paced ballasted railway rails with stone columns. For the first time, this study concentrated on increasing critical speed in fast trains using stone columns, with a focus on critical length. Other characteristics evaluated were extreme rail deformation and Dynamic Amplification Factor (DAF).

Yu et al. (2019) investigated genuine triaxial geogrid testing for high-speed trains. The study outlined a number of innovative tests procedures to investigate the geogrids' ability to enclose granular layers inside ballasted railway tracks running at near-crucial speeds. Ballasted railway rail specimens were exposed to integrated upright-horizontal cyclic stresses in order to investigate settling at high relative train speeds. When positioned at the ballast-sub-ballast boundary, when viewed alongside the unaltered circumstances, the geogrid improved settlement by around 35% and 10-15% when located at the sub-ballast-subgrade interface.

Babu & Sujatha (2010) used a finite element technique to investigate the track modulus analysis of a railway rail system. An inspection of a classical Indian railway track structure was conducted, with an attention on "track modulus" for Prestressed Concrete (PSC) and Wooden (WOOD) sleepers. According to Indian Railways requirements, the track was constructed of two standard-stretched rails, rail cushions, and sleepers with uniform sleeper separation, ballast, and subsoil that spanned the tracks. Finite Element replicas for 52PSC, 60PSC, 52WOOD, and 60WOOD tracks had been created for computer modelling of the dynamic behavior of a rail line.

Ferreira & Indraratna (2017) investigated the deformation and deterioration feedback of railway ballast under collision loads with artificial incorporation. The report described a laboratory investigation that investigated the displacement and degrading behavior of railway ballast under collision loading circumstances utilizing a heavy-scale fall-weight impact trial system. The consequence of artificial incorporation (such as rubber matting and geogrid fortification) on ballast reaction along repeated impact blows was investigated.

Zongqi et al. (2019) investigated the soil arching impact in a high-paced railway GRPS embankment put through extended traffic loading. A hinted-explicit transition computation technique was used in the study to forecast permanent deformation under high-cycle loading. Based on the technique, a set of mathematical simulations using finite element (FE) models were performed to look into the soil's arching impact in a Geosynthetic reinforced pile-supported (GRPS) embankment incorporated to long-term traffic loading. The results showed that under traffic loading, the extent and affected region of stress accumulation over embankment piles are both diminished.

Alabbasi & Hussein (2021) investigated the geo-mechanical modeling of railway ballast. Recognising the mechanical exploits of railway ballast allows for better depiction and servicing. Two methodologies were used in the literature to research the mechanical behaviour of railway ballast: large-scale testing and simulation. The goal of this work was to perform a review of the literature on modelling approaches used for analysing ballast mechanical actions.

Yetimoglu et al. (1994) inspected the loading capability of rectangular footings on geogrid-strengthened sand. Practical model experiments and finite-element calculations were used to study the loading capability of rectangular foundations on geogrid-strengthened sand. The loading capability was evaluated based on the extent of the first reinforcement layer, the vertical distribution of reinforcement sections, the amount of reinforcement sections, and the proportion of the reinforcement sheet. When single-layer reinforcement was utilized, both practical and quantitative evaluations demonstrated that the bearing ability was highest at the optimal reinforcing embedment depth. Furthermore, an ideal reinforcing spacing for multi-layer reinforced sand appeared to exist.

Leshchinsky & Ling (2013) inspected the effects of geocell curtailment on the firmness and deformation behavior of gravel. A series of embankment simulation experiments with various geocell deployment configurations were performed to inspect the influence of geocell restriction on substructure stability (one layer and two layers of geocell) were built and compared to unreinforced control tests, loaded monotonically and cyclically. After these tests were completed, the simulated embankments were mathematically modelled using finite-element methods. The results, which were very close, were then used as justification for parametric study, which looked at the impacts of less competent geocell substance, gravel, and foundation circumstances, as well as the repercussions of those aspects.

Lenart & Klompaker (2015) studied the Geogrid strengthened railway embankment on soft soil. Geogrid or geo-composite products for reinforcement, filtration, and separation had been successfully installed in many projects as an economic measure for restoring and/or upgrading existing railway lines, and crucial characteristics for these materials had been defined by Railway Authorities. Through shear interaction, the geogrid reinforcement restricted lateral deformations of the ballast/sub-ballast, reducing permanent lateral strains and vertical stresses in the long run. As a separation and filtering layer, the geotextile component prevented the mixing of the frequently fine subgrade (clay/silt) with the coarse aggregate, preventing distortion of the entire track superstructure.

Indraratna et al. (2006) investigated the geotechnical features of ballast and the involvement of geosynthetics in rail route stability. The ballast and its engineering behavior were critical in determining the stability and performance of railway lines. Large-scale triaxial testing was used to look at the deformation and disintegration of ballast under both static and dynamic stresses. The application of different geosynthetics to improve the durability of fresh and reused ballast was also investigated. The study found that adding geosynthetics to ballasted tracks increases their performance.

Leshchinsky et al. (2016) investigated the use of microgrid inclusions to improve sand strength and stiffness. The findings and evaluation of several types of triaxial compression experiments conducted to investigate the mechanical attributes of poorly-categorized sand combined with arbitrarily-oriented, minute grid insertions ("microgrids") of varying concentrations and proportions were presented in the study. The use of moderately stiff microgrids, in conjunction with frictional contact and sand particle interlocking inside grid apertures, improved the reinforced composites' strength and stiffness at low constraints. The microgrid strengthening combination increased the soil's internal angle of friction from 50 to 100 and increased the secant rigidity by up to 50%.

Arulrajah et al. (2009) investigated ground improvement methods for railway embankments. In Peninsular Malaysia, between Rawang and Bidor, a 110-kilometer-long fast speeds railway facility with trains travelling at rates of up to 160 km/h was created. Vibro-substitution with stone pillars, wilted deep soil combining (cement columns), and geogrid-reinforced piled embankments with separate pile capping are all examples of these techniques, and removal/replacement operations were used in the project.

Esmacili et al. (2018) examined the consequence of geogrid on elevated railway embankment strengthening. Utilizing laboratory experiment and finite element technique, the research evaluated the consequence of geogrid on elevated railway embankment integrity and subsidence control. To accomplish this, five sequence of 50 cm high embankments were built at 1:20 dimension, then symmetrically loaded on the top in a 240*235*220 cm loading chamber. The strengthened embankments with a solo geogrid section experienced a 7.14% increase in bearing capacity and an 11.24% reduction in settlement.

Nayyar & Sahu (2021) studied the numerical study of a railway substructure using geocell-reinforced ballast. This research described the process of developing a analytical model of a railway substructure, with a focus on its subsoil stress behavior. The study also included a numerical comparison of subgrade pressures of railway components with unreinforced and fortified ballast. The intention of this study was to accomplish a suitable interpretation of how stress is dispersed in railway components with and without strengthening as a result of train movement.

Leshchinsky & Ling (2013) investigated the numerical adapting of the behavior of a railway ballasted construction with geocell internment. The intent of the study was to assess the effects of geocell isolation on ballasted embankments when they came into a loose subgrade, thinner ballast, or varying reinforcement stiffnesses. Based on the investigation, when used over a wide variety of subgrade stiffnesses and with lesser ballast, geocell confinement might provide significant benefits.

Sowmiya et al. (2010) studied the 3D structured Finite-Element Evaluation of Railway Tracks. To upgrade the tracks with the present traffic conditions, new design approaches, and parametric studies were required to study the influence on the track system. The geotechnical and tunneling program MIDAS (GTS) was used to construct three-dimensional finite element models for this purpose. The displacement and vertical tension along the track components were predicted using a finite element model.

2.2 RESEARCH GAP

On the basis of the literature survey, it was concluded that the dynamic behavior of moving load is different from static behavior. The momentum of the mobile load and the time interval are the major factors influencing the railway formation system. Geosynthetic installment techniques also influence the distribution of transferred stress and deformation characteristics. Researchers tried to simulate the moving load on different software but limited studies have been done related to high-speed trains (i.e., Speed>250 km/hr.).

CHAPTER 3

METHODOLOGY

3.1 GENERAL

An overview of railway formation, geosynthetic materials, and finite element technique has been intimated in the aforementioned chapters. The basic objective of the present analysis is to model a railway formation simulating the real-time moving load condition. To achieve the stated objective the following flow chart will be followed.

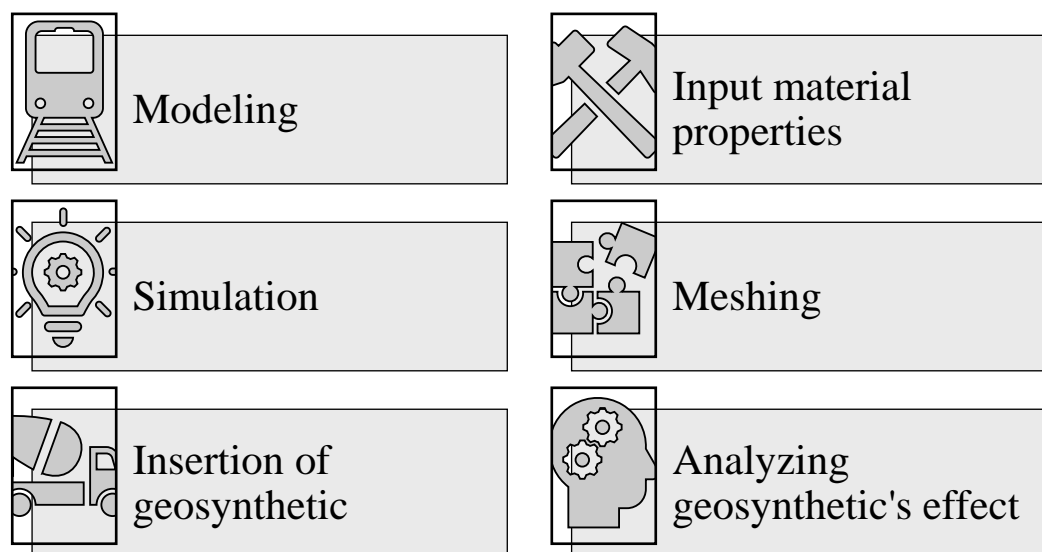


Fig 3.1 Flow chart of the methodology

3.2 MODELING

Fig.3.2 shows the railway formation that is taken into consideration for this study. The part has the following measurements: 35 m x 35 m x 9.5 m. The ballast layer is 350 mm thick, while the blanket layer is 600 mm thick. According to RDSO (2018) recommendations, a slope of 2H:1V is used (Fig 3.3).

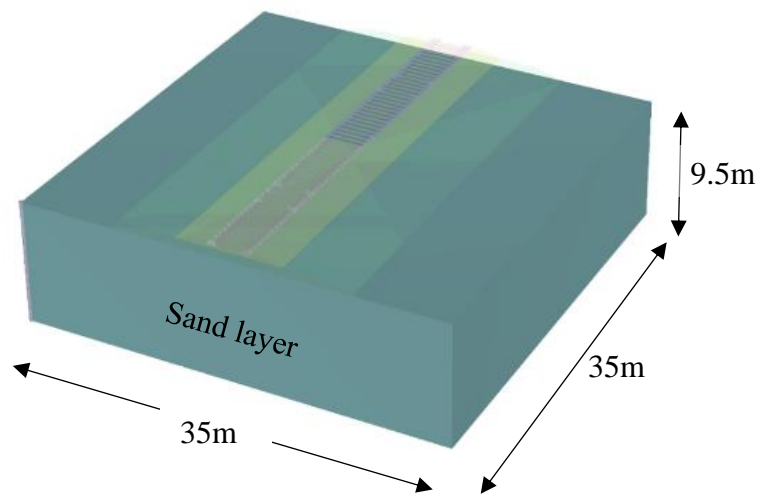


Fig. 3.2 Dimensions of the Numerical Model

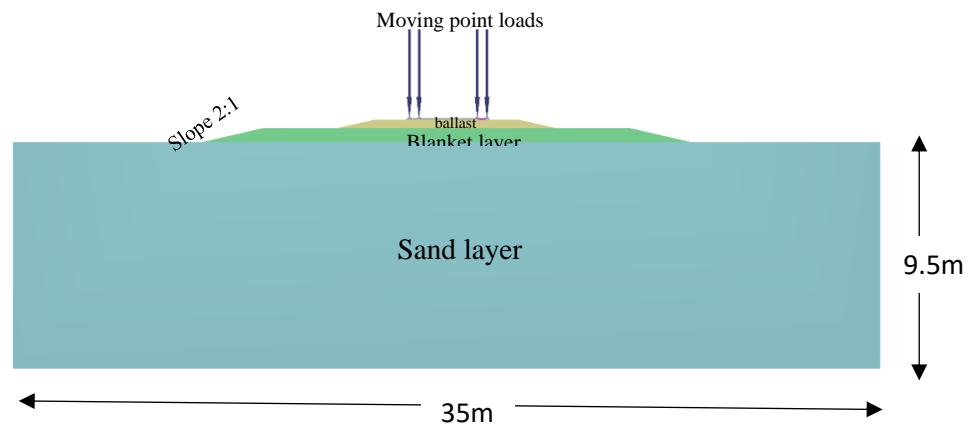


Fig. 3.3 Railway section for the modeling

3.3 MATERIAL PROPERTIES

Tables 3.1 and 3.2 provide a list of the mechanical properties of railway materials as well as the characteristics of various materials employed in the simulation process.

Table 3.1 Basic material characteristics of the soil layers for LE and MC models*

S.No.	Soil layers	γ_{sat} (kN/m ³)	γ_{unsat} (kN/m ³)	μ	ϕ (degree)	c (kN/m ²)	Ψ (degree)	E (kN/m ²)
1	Ballast	21	19	0.3	65*	31*	5	110000*
2	Blanket	23	22	0.25	40	30	15	55000
3	Sand	20	19	0.35	40	5	10	80000

*Shahraki et al. (2014)

Table 3.2 Input properties in PLAXIS 3D for rail and sleeper*

Parameter	Rails	Sleepers
Cross section area (A) [m ²]	7.7*10 ²	5.13*10 ²
Unit weight [kN/m ³]	78	25
Young's modulus (E) [kN/m ²]	200*10 ⁶	36*10 ⁶
Moment of inertia around the second axis (I ₃) [m ⁴]	3.055*10 ⁻⁵	0.0253
Moment of inertia around the third axis (I ₂) [m ⁴]	5.13*10 ⁻⁶	2.45*10 ⁻⁴

*Shahraki et al. (2014)

3.3.1 GEOGRIDS

By improving the rigidity of the base and resisting deformations, geogrids allow a homogeneous distribution of loads across a greater area. The geogrid utilized in this case is a uniaxial geogrid, which is a planar geogrid with greater strength in one direction. Geogrid characteristics are extracted from RDSO recommendations. Table 3.3 provides the specifications and laying parameters of geogrids. For the simulation procedure, two models are constructed. The geogrid is positioned at the interface between the blanket layer and the ballast in the first model. In the second model, the ballast layer is reinforced by geogrids at 0.1 m intervals, and one layer is inserted below the blanket layer for extra reinforcement.

Table 3.3 Properties of Geogrids

Mechanical Properties	Test Method	Value
Ultimate Tensile Strength: (i) For use in/below the bottom of the ballast (ii) For use in the blanket/prepared subgrade/ subgrade layer	ASTM D6637- 2015	30 kN/m (MD) 30 KN/m (CD) 20 kN/m (MD) 20 kN/m (CD)
Strain at Ultimate Tensile Strength		8- 12%

3.4 SIMULATION

3.4.1 PLAXIS 3D

PLAXIS 3D offers the most important capability for performing common soil and rock deformation and safety analyses. This complete software for the design and study of soils, rocks, and related structures allows for full 3D modeling. PLAXIS 3D provides many calculation types to satisfy the particular geotechnical issues of soil structure interactions, such as plastic, consolidation, and safety analysis. A variety of material models for forecasting the behavior of various soil and rock types are available.

PLAXIS 3D has the following input parameters:

- *Soil* is the first input parameter that defines the dimensions and materials of the borehole. Different layers of soil can be defined by inputting basic values like cohesion, angle of friction, density, etc.
- *Structures* define the whole geometry of the model. The whole model is created here by inputting the values of loads, beams, layers, and materials.
- *Mesh* divides the whole geometry into small and finite numbers of elements and nodes. A particular element or node can be chosen for the calculation process.
- *Flow conditions* define the flow to pore water in the structure. The basic flow conditions can be controlled here.
- *Staged construction* splits the geometry into phases. For example, if we try to analyze the effect of geosynthetics before and after loading, it can be done into phases by this parameter.

3.4.2 FINITE ELEMENT MODEL

For modeling, an ICE train model is used, which is an intercity express train that is commonly used in Germany. Table 3.4 lists the requirements utilized in the modeling. Figure 3.4 depicts the dimensions of an ICE train as well as the predicted lengths for the model.

Table 3.4 Model parameters for modeling the moving loads*

Distance between the first and the last wagon axles [m]	21.7
Additional length for model [m]	6.5
Total additional length (right and left) [m]	13.0
Model length [m]	34.7
Sleeper distance [m]	0.6
Dynamic loads distance [m]	0.3

*Shahraki et al. (2014)

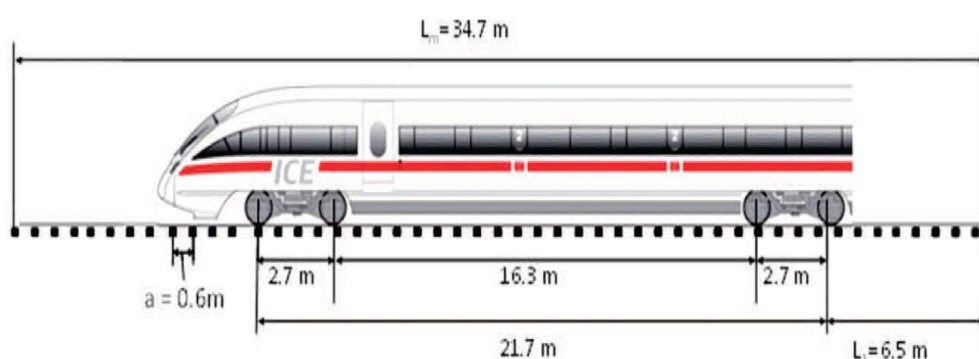


Fig. 3.4 Dimensions of an ICE train and calculated lengths for model

Fig 3.5 illustrates the finite model of the ICE train. The dimensions are taken as per the table given above. The model is placed and spaced after considering the total track length and the time taken by the model to cover that distance.

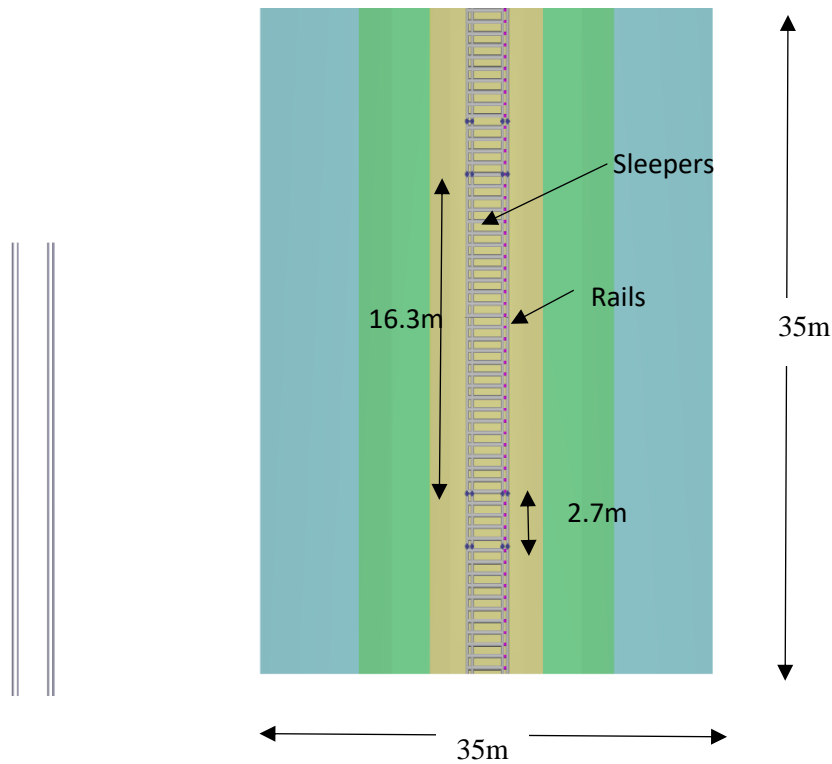


Fig. 3.5 Finite Element model of ICE train

For the simulation procedure, two models are constructed. The geogrid is positioned at the intersection between the blanket layer and the ballast in the first model. The first model is analyzed at the speeds of 180 km/h and 360 km/h. In the second model, the ballast layer is reinforced by geogrids at 0.1 m intervals, and one layer is inserted below the blanket layer for extra reinforcement.

3.4.3 LOADING

The rails and sleepers were built with elastic materials. The train loads at the rail were approximated using a moving point load. The section traveled at speeds of 180 km/hr and 360 km/hr while experiencing an axle-applied wheel force of 90 kN. Figure 3.6 displays the organization of the axial load.

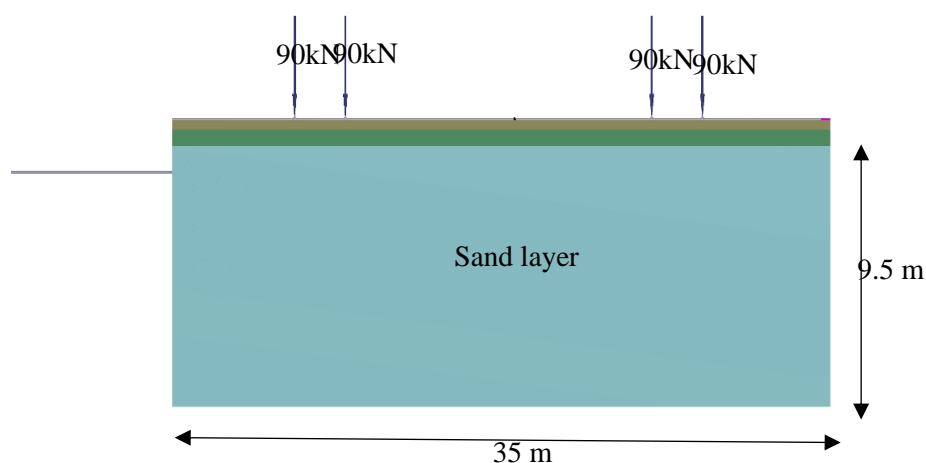


Fig. 3.6 Illustration of loading

The whole length of the track was determined to be 35 m. The train's journey time to pass this portion at 180 km/h was 0.7 sec, and at 360 km/h was 0.35 sec however considering the whole dimension of the train, the duration was reduced to 1 sec (180 km/h) and 0.5 sec (360 km/h) for dynamic study. To make the computation procedure easier, the time taken was broken into 20 sub-steps.

3.5 MESHING

To represent the segment, 10-noded elements were used. For this objective, two models are simulated. For both models, the mesh size was set to very coarse. In the initial model, the amount of soil components was 2660, and the number of nodes was 4856. The element size was 2.762 m on average. The largest element size was 10.45 m, while the smallest was 2.00×10^{-3} m. In the second model, the amount of soil components was 4617, and the number of nodes was 7983. The element size was 2.416 m on average. The largest element size was 10.06 m, while the smallest was 2.079×10^{-3} m.

Elements and nodes are described in Fig. 3.7 and Fig. 3.8 respectively.

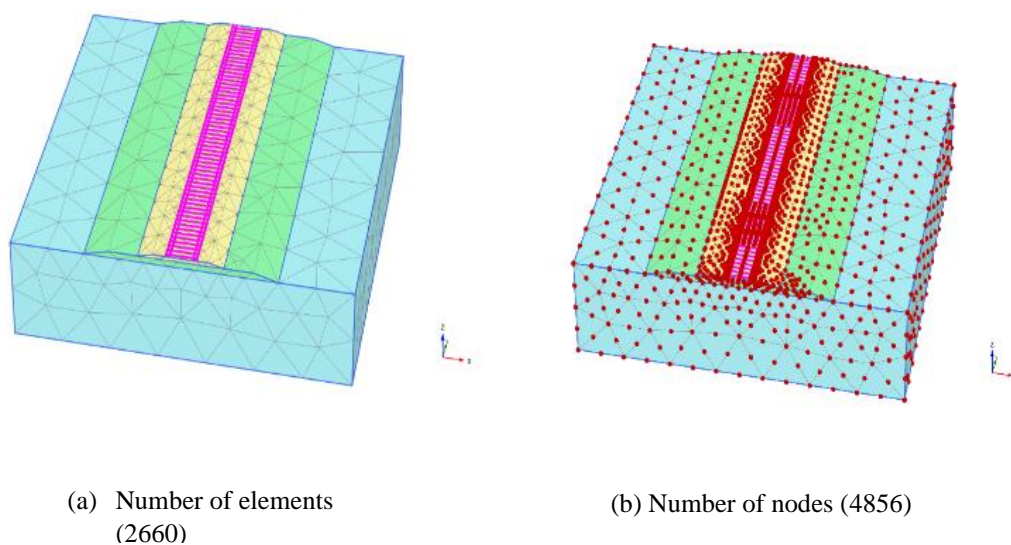


Fig. 3.7 Elements and Nodes for Model 1

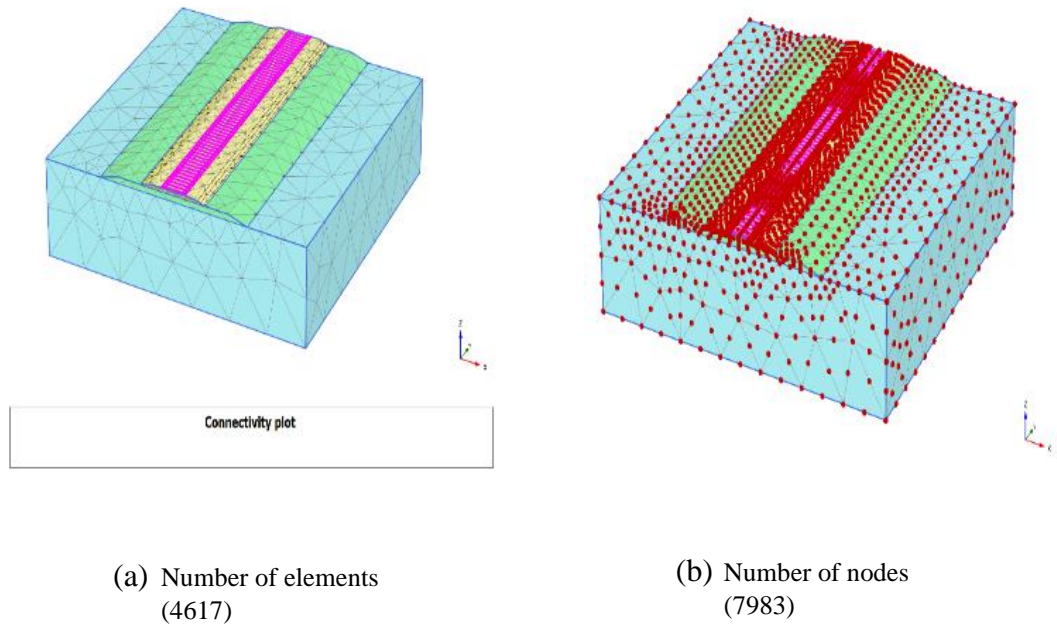


Fig. 3.8 Elements and Nodes for Model 2

CHAPTER 4

RESULTS AND DISCUSSION

4.1 GENERAL

Under time-dependent stresses, dynamic analysis is utilized to estimate stress, strain, and deformation. Dynamic examination is further accurate than static examination which does not consider the time dependency of the loads. Although dynamic examination is more sophisticated than static examination but gives more precise results than static examination. In this study, the major factors that are analyzed are deformations and stress in different directions.

4.2 For Model 1

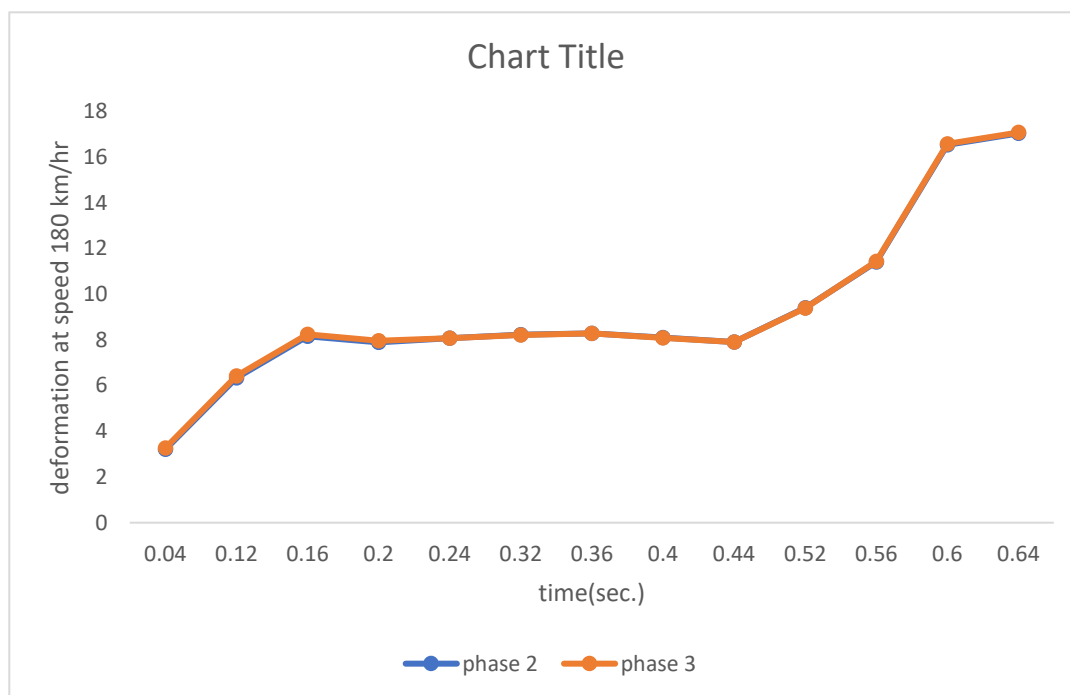
4.2.1 VERTICAL DEFORMATIONS

In the first model, the geogrid is inserted at the boundary of the blanket layer and the ballast. Only a single layer of geogrid is applied to check the deformation properties. It incorporates of two phases. In the first phase, loading is applied for different speeds without the geogrids being activated. In the second phase, the geogrids are activated and their effect is then analyzed. Table 4.1 listed the deformation in the z-direction for different speeds of 180 km/h and 360 km/h. Fig 4.1 and Fig 4.2 show the graph between deformation and the time interval for different phases. Fig 4.3 and Fig. 4.4 show the simulation output of PLAXIS 3D.

Table 4.1 Deformations in the Z-direction with and without geogrid

Time	Phase 2* (180km/hr.)	Phase 3* (180km/hr.)	Time	Phase 2* (360km/hr.)	Phase 3* (360km/hr.)
(sec.)	Max. (10^{-3})	Max. (10^{-3})	(sec.)	Max. (10^{-3})	Max. (10^{-3})
0.04	3.205	3.268	0.025	4.790	4.853
0.12	6.340	6.419	0.05	8.973	9.053
0.16	8.161	8.239	0.075	14.43	14.64
0.20	7.883	7.956	0.10	17.54	17.87
0.24	8.070	8.071	0.150	27.37	27.44
0.32	8.219	8.217	0.20	27.78	27.82
0.36	8.281	8.275	0.250	34.25	34.47
0.40	8.10	8.091	0.275	40.80	41.65
0.44	7.908	7.901	0.30	47.21	47.41
0.52	9.398	9.388	0.325	55.20	55.35
0.56	11.41	11.43	0.35	57.66	57.83
0.60	16.53	16.57	0.375	57.37	57.52
0.64	17.03	17.07	0.40	57.15	57.28

*Phase 2: without geogrid *Phase 3: with geogrid

**Fig 4.1 Graph between deformation and time at speed 180 km/hr.**

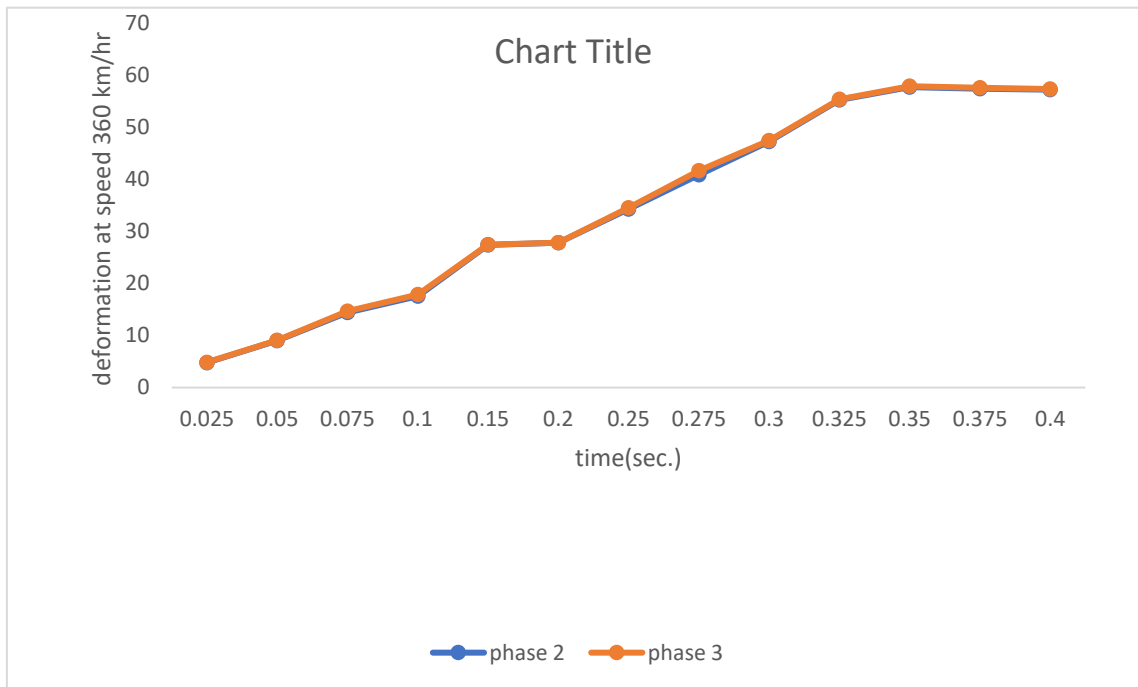


Fig 4.2 Graph between deformation and time at 360 km/hr.

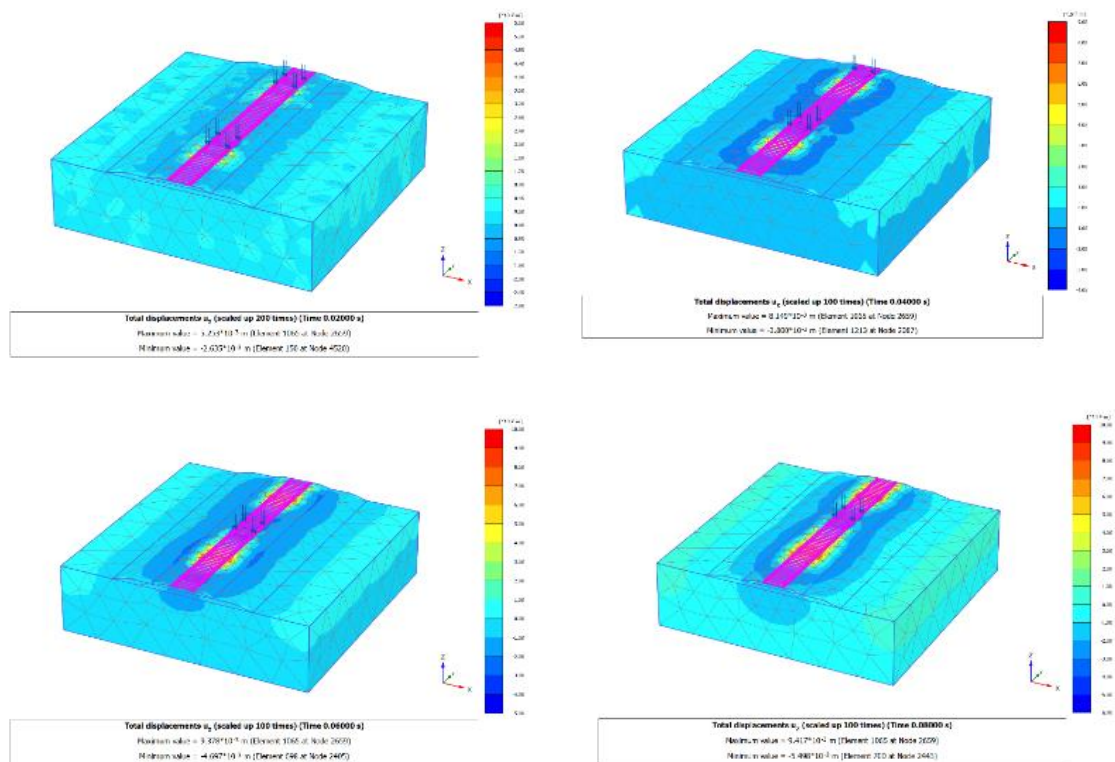


Fig. 4.3 Total displacements at different intervals without the geogrid

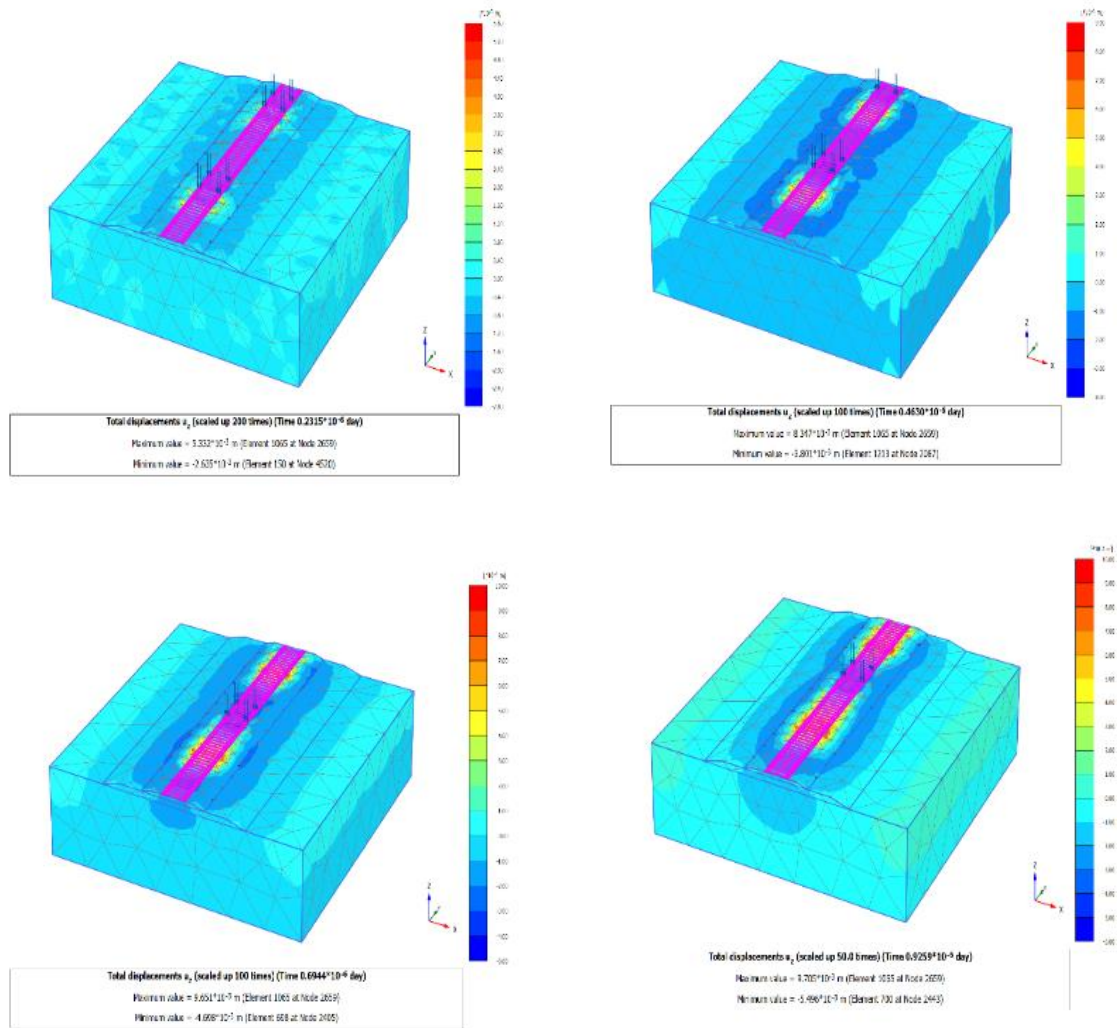


Fig. 4.4 Total displacements at different intervals with the geogrid

Table 4.2 shows the deformation in the Y-direction with and without geogrids at different speeds of time. Fig 4.5 and Fig 4.6 show the graph between deformation and the time interval.

Table 4.2 Deformations in the Y-direction with and without geogrid

Time (sec.)	Phase 2* (180km/hr.) Max.(10 ⁻³ m)	Phase 3* (180km/hr.) Max. (10 ⁻³ m)	Time (sec.)	Phase 2* (360km/hr.) Max.(10 ⁻³ m)	Phase 3* (360km/hr.) Max.(10 ⁻³ m)
0.04	0.4798	0.4794	0.025	0.4423	0.4423
0.12	1.233	1.233	0.05	0.8255	0.8223
0.16	2.651	2.639	0.075	1.236	1.227
0.20	3.985	3.967	0.10	4.201	4.199
0.24	4.520	4.501	0.150	7.984	7.943
0.32	4.959	4.932	0.20	8.267	8.214
0.36	4.995	4.968	0.250	8.484	8.438
0.40	4.883	4.853	0.275	11.20	11.17
0.44	4.883	4.848	0.30	14.21	14.19
0.52	6.112	6.080	0.325	16.08	16.04
0.56	7.166	7.125	0.35	16.61	16.61
0.60	8.497	8.445	0.375	16.75	16.78
0.64	8.713	8.663	0.40	16.80	16.83

*Phase 2: without geogrid *Phase 3: with geogrid

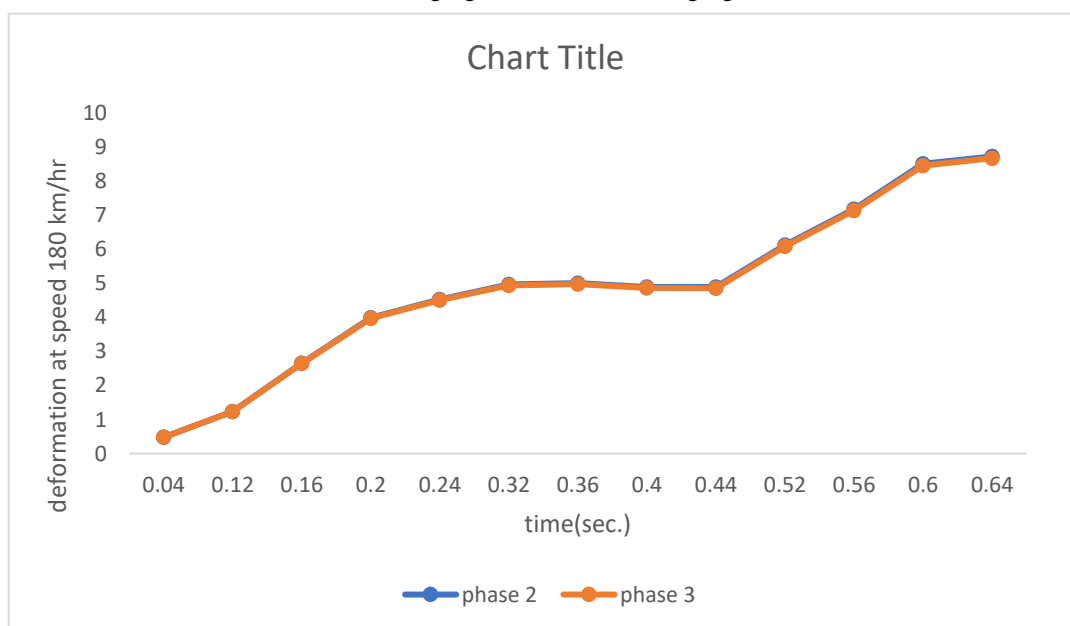


Fig 4.5 Graph between deformation and time at speed 180 km/hr.

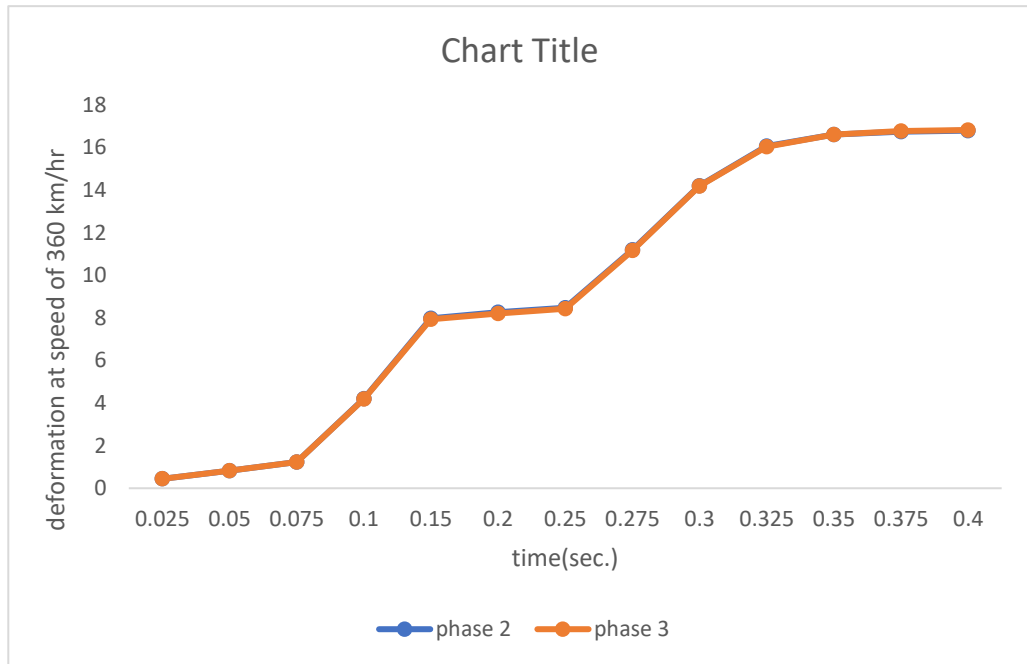


Fig 4.6 Graph between deformation and time at speed 360 km/hr.

4.2.2 DISPLACEMENTS AND STRESSES IN THE RAIL SECTION

Figure 4.7 depicts the axial forces and displacements in the rail segment. Figure 4.8 shows that geogrids increase the distribution of axial forces in the rail section at certain points, while they are ineffective at others.

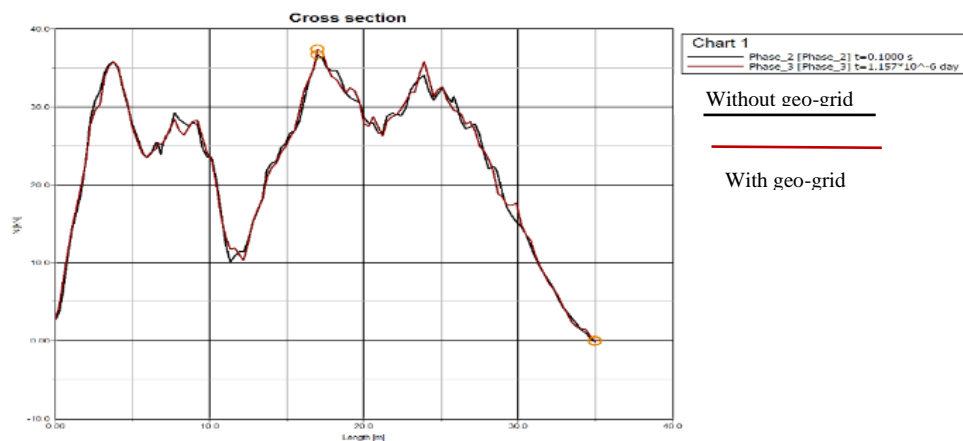


Fig 4.7 Axial force(kN) and the cross-section of the rail (m)

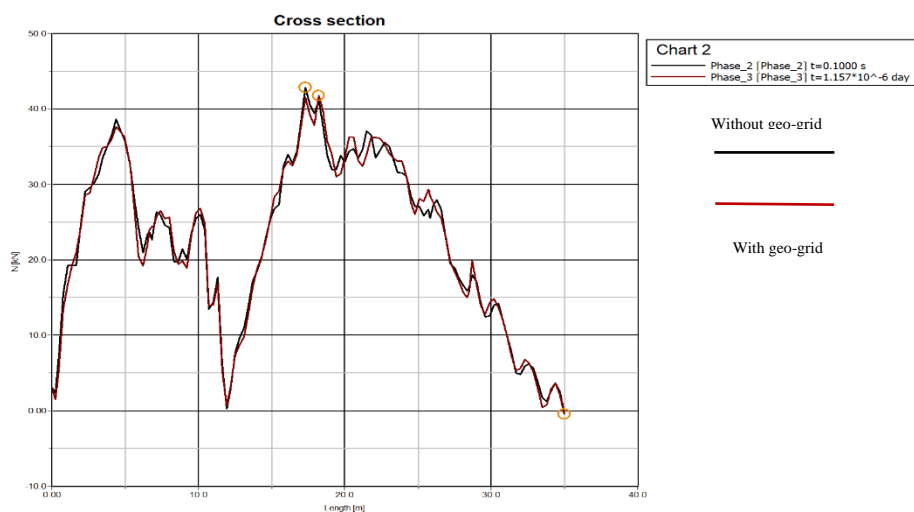


Fig 4.8 Axial force(kN) and the cross-section of the rail (m)

Figure 4.9 depicts the relationship between Y-direction displacement and rail section length. Geogrids serve to control axial deformations since they are axial members that can only accept tension and not compression. The displacement in the z-direction is seen in Fig.4.10. After employing the geo-grid, there is simply any substantial change in the value. This might be connected to the axial rigidity of the geogrid and the train's movement direction.



Fig 4.9 Plot between displacement(m) and cross-section of the rail (m)

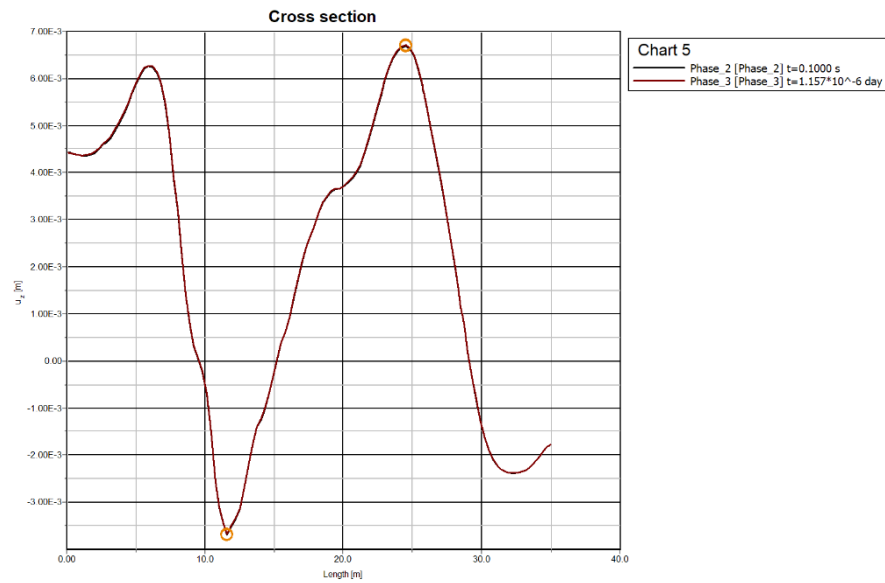


Fig 4.10 Plot between displacement(m) and cross-section of the rail (m)

Fig .4.11 and Fig 4.12 show the plot between shear forces in the x-y direction and the x-z direction. As per the graph when the train is between the length 0-10m it experiences the maximum shear force because the full load is experienced by the section at that time. As the train passes the section the load decreases hence the values of shear force also decrease in the coming section.

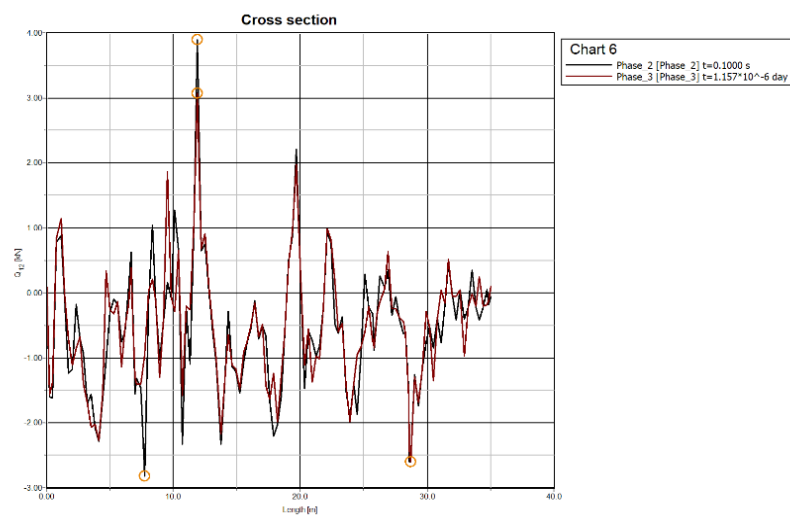


Fig 4.11 Shear forces in the x-y direction

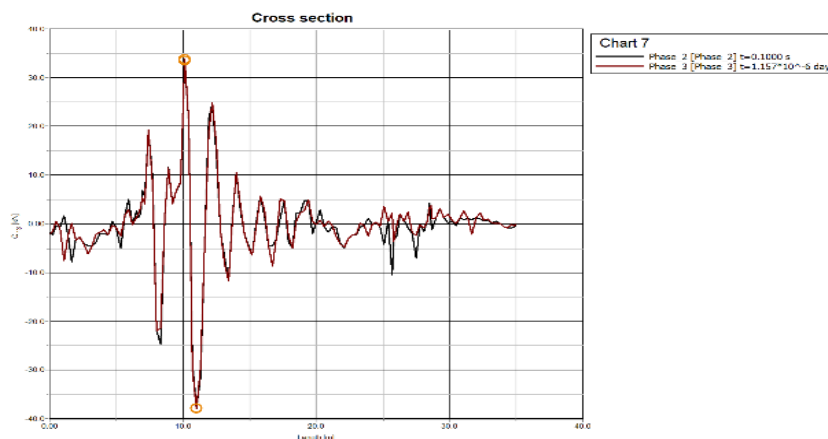


Fig 4.12 Shear forces in the x-z direction

4.3 FOR MODEL 2

4.3.1 VERTICAL DEFORMATIONS

In the second model, the geogrids are inserted in the ballast at spacings of 100cm. in comparison to the first model, the second model is more reinforced and is analyzed for deformations and stress. Model 2 also includes two stages. Moving loads are applied without the usage of the geogrid reinforcement during the first phase, and the geogrid is activated during the second phase. The simulation results in deformations, stresses, and shear forces at various places and cross-sections of the model. Figures 4.13 and 4.14 show the total displacements in the z-direction at time 0.1 seconds with and without the inclusion of the geogrid, respectively.

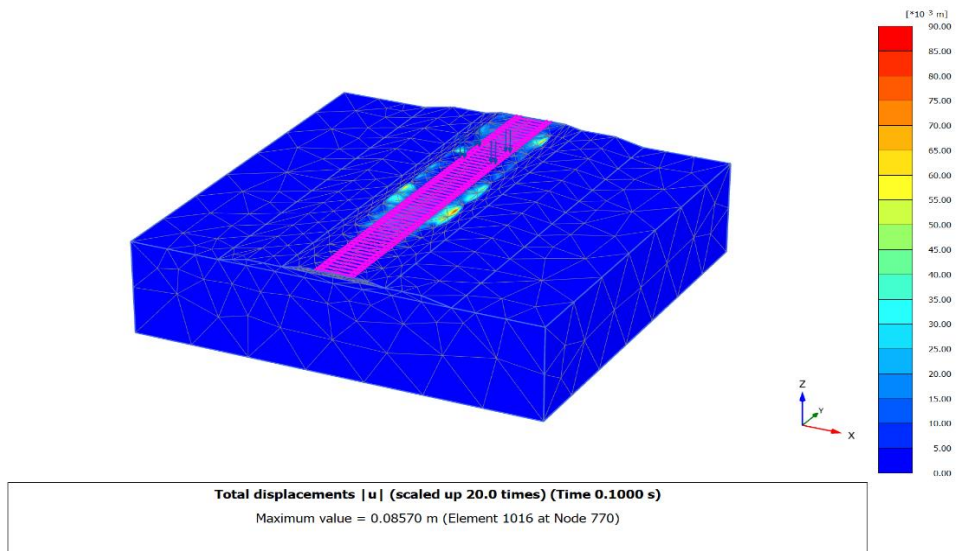


Fig. 4.13 Total displacement without the geogrid

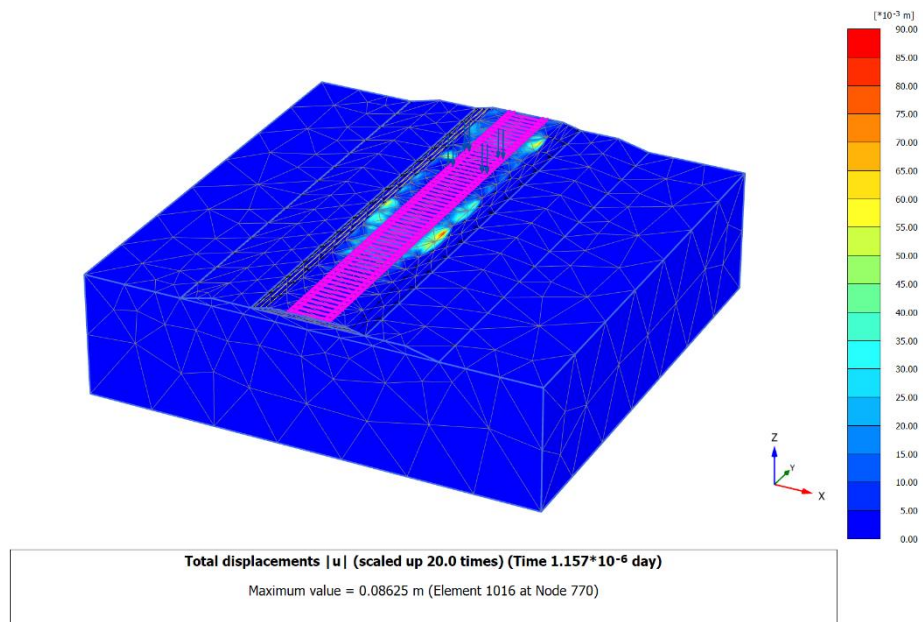


Fig. 4.14 Total displacements with the geogrid

Figures 4.15 and 4.16 show the total displacements in the Y-direction at time 0.1 seconds with and without the inclusion of the geogrid, respectively.

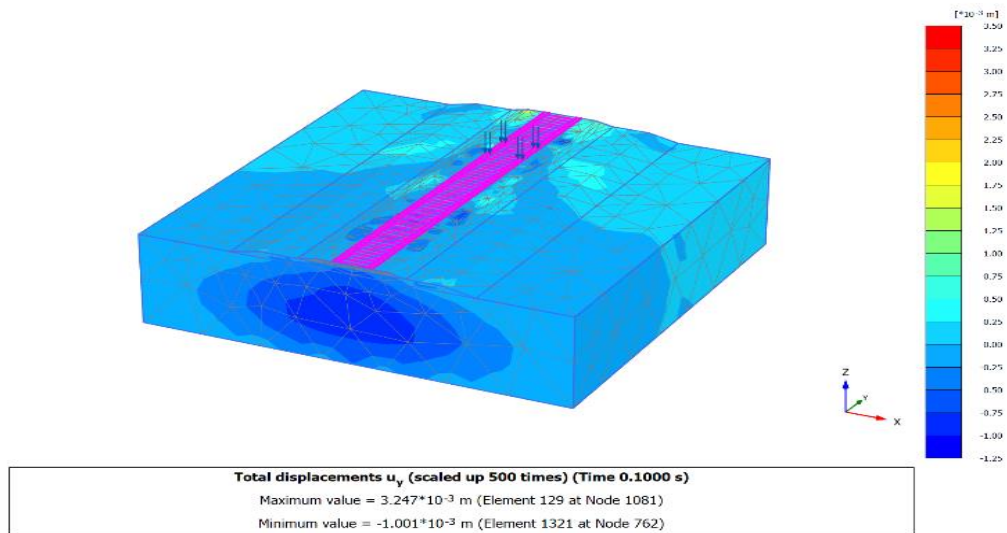


Fig. 4.15 Total displacement without the geogrid

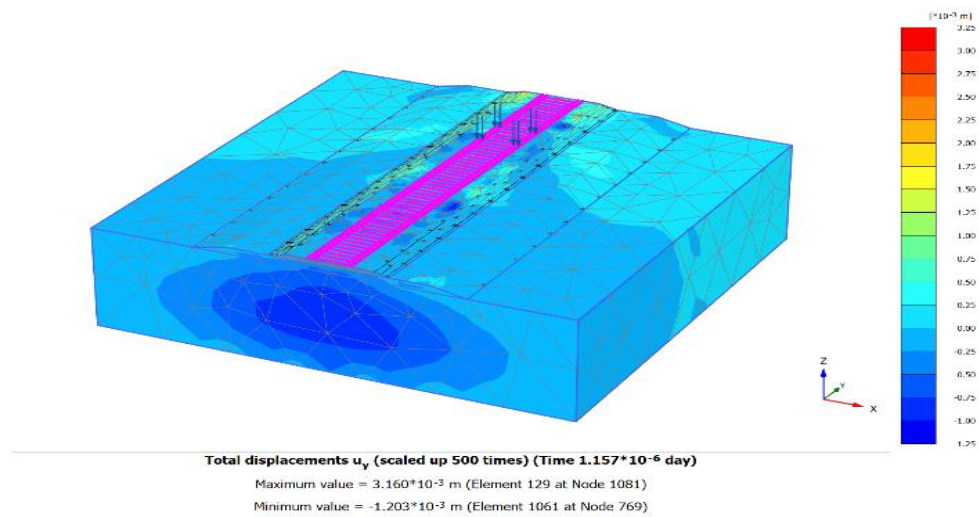


Fig. 4.16 Total displacement with the geogrid

4.3.2 STRESSES IN THE SECTION

The vertical stress at time =0.1 sec is illustrated in Fig. 4.17 In Fig. 4.17 and Fig. 4.18 it is evident that the geogrid improves the distribution of vertical stress and the value of stress is reduced by 30 % after using the geogrid in the model 2.

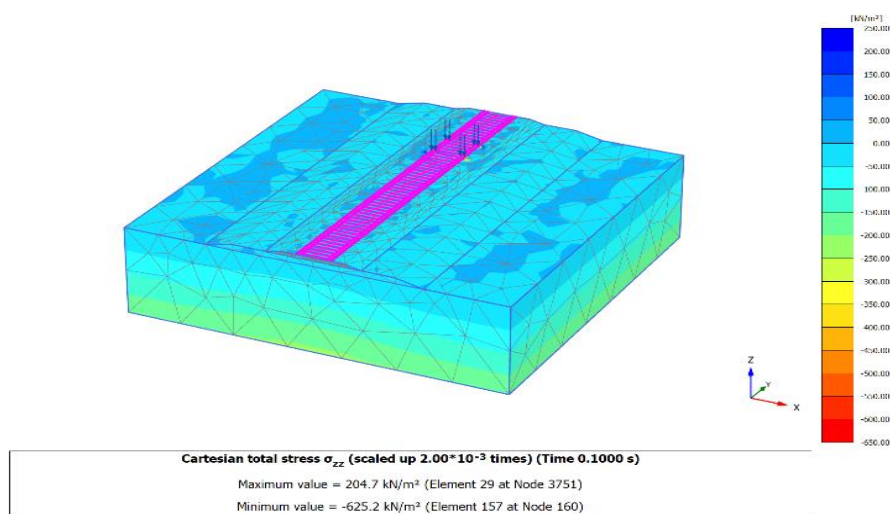


Fig. 4.17 Vertical stress at time=0.1 sec without the geogrid

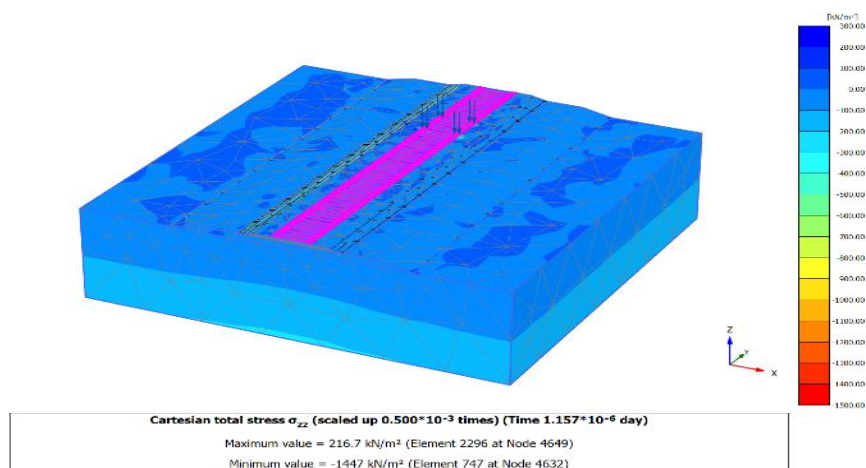


Fig. 4.18 Vertical stress at time=0.1 sec with the geogrid

4.3.3 DISPLACEMENTS AND STRESSES IN THE RAIL SECTION

Fig. 4.19 depicts the axial forces and displacements in the rail segment. Figures 4.20 and 4.21 show that geogrids increase the distribution of axial forces in the rail section at certain points, while they are ineffective at others. Figures 4.21 and 4.22 depict the relationship between Y-direction displacement and rail section length. The use of geogrids significantly reduces displacement.

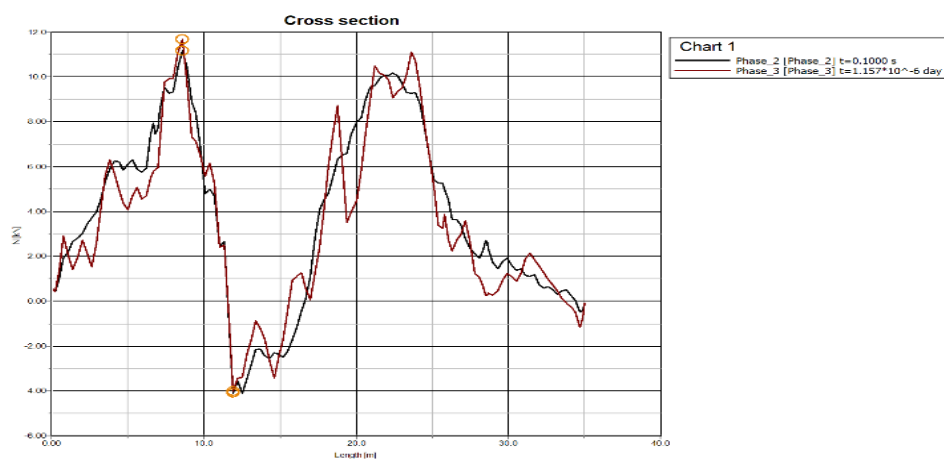


Fig 4.19 Plot between axial force(kN) and cross-section of the rail (m)

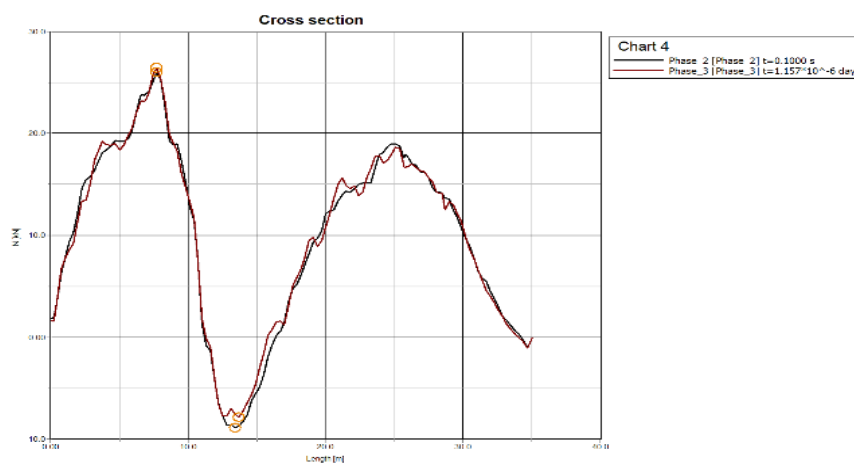


Fig 4.20 Plot between axial force(kN) and cross-section of the rail (m)



Fig.4.21 Plot between displacement(m) and cross-section of the rail (m)

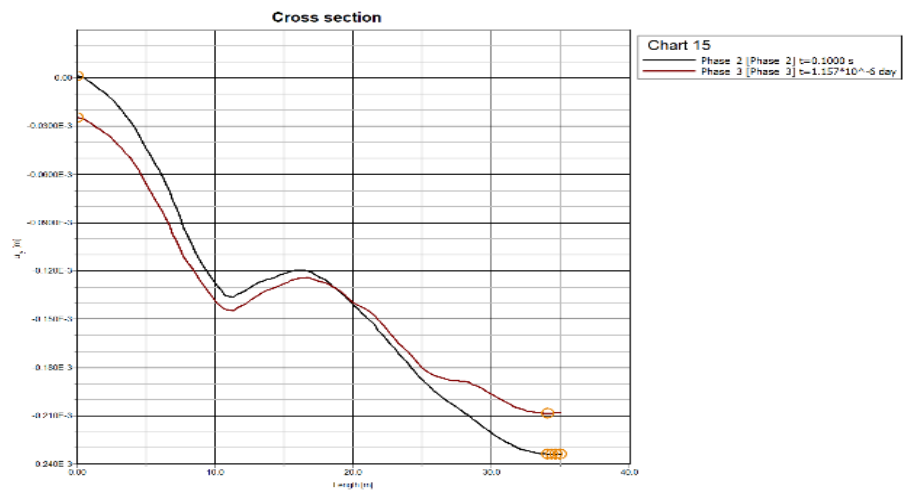


Fig.4.22 Plot between displacement(m) and cross-section of the rail (m)

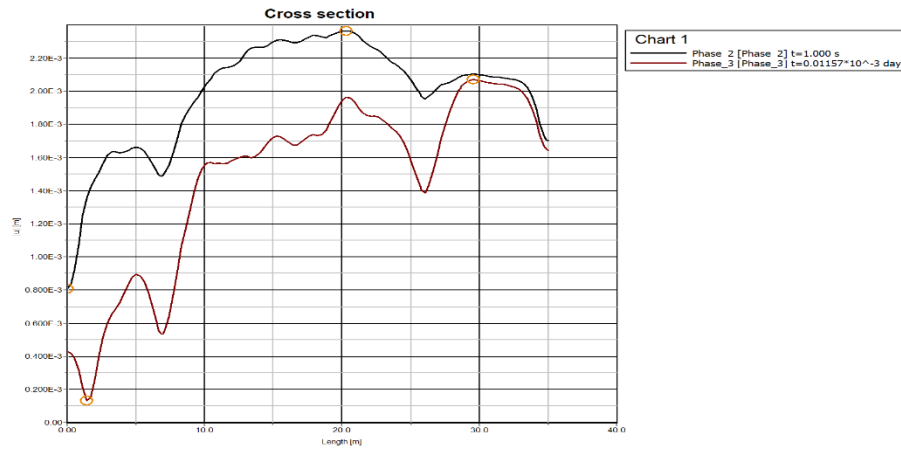


Fig.4.23 Plot between total displacement(m) and cross-section of the rail (m) at speed 180 km/h.

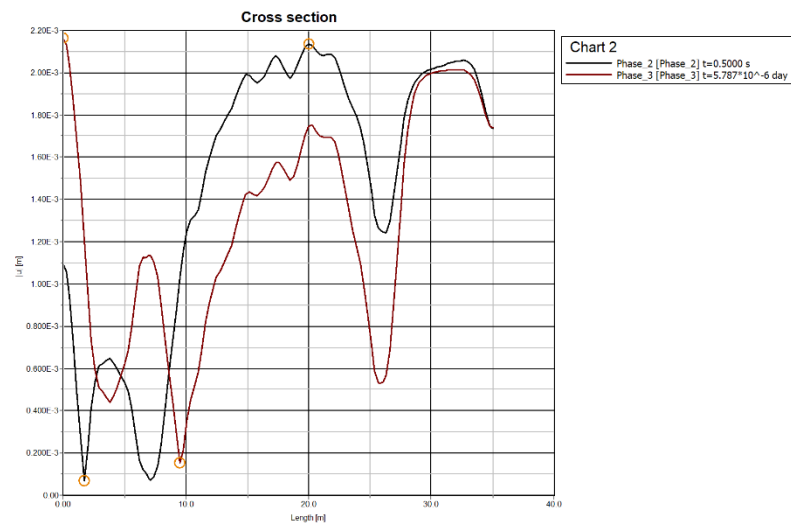


Fig.4.24 Plot between total displacement(m) and cross-section of the rail (m) at speed 360 km/h.

CHAPTER 5

CONCLUSION

For varying running speeds of 180 km/h and 360 km/h, a 90 kN moving train load was modeled using three-dimensional finite element modeling. The PLAXIS 3D programs were used to model real-time scenarios and determine deformations and stresses in the railway embankment with and without geogrid. The outcomes were predicted using dynamic analysis. After analyzing both models, it was determined that utilizing geogrid solely at the interface of the blanket layer and the ballast did not appreciably limit deformation and stresses, but there was a uniform distribution of loads in both the Y and z directions. In model 2 geogrids are installed at a spacing of 100cm in the ballast. Model 2 significantly outperformed Model 1. The use of geogrids at various depths in the ballast layer did help to control the deformation, and the stresses in the Y-direction were reduced by roughly 30%.

Following an examination of both models, the following results were reached:

- The deformations and strains grew as the train's speed rose.
- Geogrid was beneficial in limiting Y-direction deformations, but there was only a little modification in the Z-direction.
- Geogrid proved useful at a speed of 180 km/h, but as the speed grew, not many modifications were seen with the incorporation of Geogrid.
- The axial rigidity of Geogrid is critical in determining deformation and stress.
- Geogrids increase the distribution of axial forces in the rail section at certain points, while they are ineffective at others.

It is advised that after witnessing the modeling, various lab and field experiments be performed to accurately understand the results. The applicability of Geogrid can be correctly determined after the testing since Geogrid qualities are dependent on numerous aspects.

REFERENCES

1. T. Abadi, L. L. Pen, A. Zervos, and W. Powrie, “Effect of Sleeper Interventions on Railway Track Performance,” *Journal of Geotechnical and Geoenvironmental Engineering*, vol. 145, no. 4, p. 04019009, Apr. 2019, doi: [https://doi.org/10.1061/\(asce\)gt.1943-5606.0002022](https://doi.org/10.1061/(asce)gt.1943-5606.0002022).
2. Alabbasi, Y., Hussein, M., 2021 “Geomechanical Modelling of Railroad Ballast: A Review” *Archives of Computational Methods in Engineering* 2021 28, 815–839
3. Arulrajah, A. Abdullah, M. W. Bo, and A. Bouazza, “Ground improvement techniques for railway embankments,” *Proceedings of the Institution of Civil Engineers - Ground Improvement*, vol. 162, no. 1, pp. 3–14, Feb. 2009, doi: <https://doi.org/10.1680/grim.2009.162.1.3>.
4. R. P. Chen, P. Jiang, X. W. Ye, and X. C. Bian, “Probabilistic Analytical Model for Settlement Risk Assessment of High-Speed Railway Subgrade,” *Journal of Performance of Constructed Facilities*, vol. 30, no. 3, p. 04015047, Jun. 2016, doi: [https://doi.org/10.1061/\(asce\)cf.1943-5509.0000789](https://doi.org/10.1061/(asce)cf.1943-5509.0000789).
5. Esmaeili, M., Naderi, B., Neyestanaki, H.K., Khodaverdian, A. “Investigating the effect of geogrid on stabilization of high railway embankments Soils Found.”, 2018 <https://doi.org/10.1016/j.sandf.2018.02.005>
6. W. Ferdous, A. Manalo, G. Van Erp, T. Aravinthan, and K. Ghabraie, “Evaluation of an Innovative Composite Railway Sleeper for a Narrow-Gauge Track under Static Load,” *Journal of Composites for Construction*, vol. 22, no. 2, Apr. 2018, doi: [https://doi.org/10.1061/\(asce\)cc.1943-5614.0000833](https://doi.org/10.1061/(asce)cc.1943-5614.0000833).

7. India. Railway Board, *Indian Railway Code for the Engineering Department*. 1982.
8. Indraratna, B., Khabbaz, H., Salim, W. and Christie, D. (2006) “Geotechnical properties of ballast and the role of geosynthetics in rail track stabilisation” *Ground Improvement* 2006 10, No. 3, 91–101
9. R. M. Koerner, *Designing with Geosynthetics*. 2005.
10. Lenart, S., Klompaker, J. “Geogrid reinforced railway embankment on soft soil” – *Experiences from 5 years of field monitoring* 2015
<https://www.researchgate.net/publication/281117609>
11. W. Leng, Y. Xiao, R. Nie, W. Zhou, and W. Liu, “Investigating Strength and Deformation Characteristics of Heavy-Haul Railway Embankment Materials Using Large-Scale Undrained Cyclic Triaxial Tests,” *International Journal of Geomechanics*, vol. 17, no. 9, p. 04017074, Sep. 2017, doi: [https://doi.org/10.1061/\(asce\)gm.1943-5622.0000956](https://doi.org/10.1061/(asce)gm.1943-5622.0000956).
12. B. Leshchinsky and H. Ling, “Effects of Geocell Confinement on Strength and Deformation Behavior of Gravel,” *Journal of Geotechnical and Geoenvironmental Engineering*, vol. 139, no. 2, pp. 340–352, Feb. 2013, doi: [https://doi.org/10.1061/\(asce\)gt.1943-5606.0000757](https://doi.org/10.1061/(asce)gt.1943-5606.0000757).
13. B. Leshchinsky, T. M. Evans, and J. Vesper, “Microgrid inclusions to increase the strength and stiffness of sand,” *Geotextiles and Geomembranes*, vol. 44, no. 2, pp. 170–177, Apr. 2016, doi: <https://doi.org/10.1016/j.geotexmem.2015.08.003>.
14. B. Leshchinsky and H. I. Ling, “Numerical modeling of behavior of railway ballasted structure with geocell confinement,” *Geotextiles and Geomembranes*, vol. 36, pp. 33–43, Feb. 2013, doi: <https://doi.org/10.1016/j.geotexmem.2012.10.006>.

15. J. S. Mundrey, *Railway track engineering*. New Delhi, India: Mcgraw Hill Education, 2010.
16. S. Nayyar and A. K. Sahu, “Numerical analysis of railway substructure with geocell-reinforced ballast,” *Geomechanics and Geoengineering*, pp. 1–11, May 2021, doi: <https://doi.org/10.1080/17486025.2021.1928770>.
17. PLAXIS 3D Reference Manual 2020
18. PLAXIS 3D Tutorial Manual 2020
19. RDSO 1972- Civil Engineering Report no: C-127-Report on a study of the Characteristics of Compacted and Uncompacted Expansive soils.
20. Shahraki, M., Sadaghiani, M.R.S., Witt, K.J. “3D modeling of train induced moving load on an embankment” 2014 [www.plaxis.com/plaxis bulletin](http://www.plaxis.com/plaxis_bulletin)
21. Specification for railway formation RDSO/2018/GE: IRS-0004(D)
22. Sun, Qi., Indraratna, B. and Nimbalkar, S. “Deformation and Degradation Mechanisms of Railway Ballast under high-Frequency Cyclic Loading” *journal of. Geotech. Geoenviron. Eng.* 04015056 2015 doi: 10.1061/ (ASCE)GT.1943 5606.0001375.
23. X. Zhang, C. Zhao, and W. Zhai, “Dynamic Behavior Analysis of High-Speed Railway Ballast under Moving Vehicle Loads Using Discrete Element Method,” *International Journal of Geomechanics*, vol. 17, no. 7, p. 04016157, Jul. 2017, doi: [https://doi.org/10.1061/\(asce\)gm.1943-5622.0000871](https://doi.org/10.1061/(asce)gm.1943-5622.0000871).

LIST OF PUBLICATIONS

Paper title	Conference	Status
NUMERICAL SIMULATION OF RAILWAY EMBANKMENT FOR DIFFERENT SPEEDS WITH APPLICATION OF GEOGRID	National Conference on Sustainable Development of Smart Cities Infrastructure (SDSCI-2023)	Published ISBN:978-93-90951-64-2
NUMERICAL ANALYSIS OF RAILWAY FORMATION WITH GEOGRID REINFORCED BALLAST AND BLANKET LAYER	International Conference on Recent Interdisciplinary Developments in Civil Engineering ICRIDC-2023	Accepted
NUMERICAL MODELING OF HIGH-SPEED RAIL FORMATION WITH GEOGRID REINFORCED BALLAST LAYER	21st Southeast Asian Geotechnical Conference and 4th AGSSEA Conference (SEAGC-AGSSEA 2023)	Accepted